Empirical macroscopic features of spatial-temporal traffic patterns at highway bottlenecks

Boris S. Kerner*
DaimlerChrysler AG, FT3/TN, HPC: E224, 70546 Stuttgart, Germany
(Received 10 October 2001; revised manuscript received 17 December 2001; published 10 April 2002)

Results of an empirical study of congested patterns measured during 1995–2001 at German highways are presented. Based on this study, various types of congested patterns at on and off ramps have been identified, their macroscopic spatial-temporal features have been derived, and an evolution of those patterns and transformations between different types of the patterns over time has been found out. It has been found that at an isolated bottleneck (a bottleneck that is far enough from other effective bottlenecks) either *the general pattern* (GP) or *the synchronized flow pattern* (SP) can be formed. In GP, synchronized flow occurs and wide moving jams spontaneously emerge in that synchronized flow. In SP, no wide moving jams emerge, i.e., SP consists of synchronized flow only. An evolution of GP into SP when the flow rate to the on ramp decreases has been found and investigated. Spatial-temporal features of complex patterns that occur if two or more effective bottlenecks exist on a highway have been found out. In particular, the *expanded pattern* where synchronized flow covers two or more effective bottlenecks can be formed. It has been found that the spatial-temporal structure of congested patterns possesses predictable, i.e., characteristic, unique, and reproducible features, for example, the most probable types of patterns that are formed at a given bottleneck. According to the empirical investigations the cases of *the weak* and *the strong* congestion should be distinguished. In contrast to the weak congestion, the strong congestion possesses the following characteristic features: (i) the flow rate in synchronized flow is self-maintaining near a limit flow rate; (ii) the mean width of the region of synchronized flow in GP does not depend on traffic demand; (iii) there is a correlation between the parameters of synchronized flow and wide moving jams: the higher the flow rate out from a wide moving jam is, the higher is the limit flow rate in the synchronized flow. The strong congestion often occurs in GP whereas the weak congestion is usual for SP. The weak congestion is often observed at off ramps whereas the strong congestion much more often occurs at on ramps. Under the weak congestion diverse transformations between different congested patterns can occur.

DOI: 10.1103/PhysRevE.65.046138 PACS number(s): 89.40.+k, 47.54.+r, 64.60.Cn, 05.65.+b

I. INTRODUCTION: OBJECTIVE CRITERIA FOR DIFFERENT PHASES IN CONGESTED TRAFFIC

Traffic on a multilane highway can be either ''free'' or ''congested'' (e.g., Refs. [1–76]). Free flow states are nearly related to a curve with a positive slope in the flow-density plane. This curve is cut off at a limit (critical) vehicle density where the related average vehicle speed reaches the minimum possible average speed in free flow (e.g., Refs. [13,28,30,54]).

Congested traffic states can be defined as the traffic states where the average vehicle speed is lower than the minimum possible average speed in free flow (e.g., Ref. [54]). In congested traffic, where a synchronization of vehicle speed on different highway lanes usually occurs [5,54] complex spatial-temporal patterns are observed, in particular a sequence of moving traffic jams, the so called ''stop-and-go'' phenomenon (e.g., the classical works by Treiterer [53] and Koshi *et al.* [54]).

It has recently been found that in congested traffic two qualitatively different traffic phases—the traffic phase ''wide moving jam'' and the traffic phase ''synchronized flow''—should be distinguished [56,66,64]. A moving jam is an upstream moving localized structure that is restricted by two fronts where the vehicle speed changes sharply. The distance between the fronts of a *wide* moving jam is noticeably higher than the widths of the jam fronts. As in synchronized flow there is usually a synchronization of the vehicle speeds on different highway lanes inside the fronts of wide moving jams. The concept of the traffic phase ''synchronized flow'' introduced by the author is based on qualitatively different *empirical spatial-temporal* features of synchronized flow in comparison with wide moving jams. Thus, objective criteria to distinguish the different phases in congested traffic are linked to the qualitatively different spatial-temporal features of these phases [56,67,68]. These objective criteria will be *defined* as the following [56,57,67,68,73].

(a) A local spatial-temporal upstream moving traffic pattern in congested regime, i.e., the pattern that is spatially restricted by two upstream moving (downstream and upstream) fronts belongs to the traffic phase ''wide moving jam,'' if at the given ''control parameters'' of traffic (e.g., the weather and other environmental conditions) the pattern possesses the following characteristic, i.e., unique, coherent, predictable, and reproducible feature. The pattern as a whole local structure propagates through any states of free and synchronized flows and through any bottlenecks (e.g., at on ramps and off ramps) *keeping* the mean velocity of the downstream front of the pattern. This velocity is the same for different wide moving jams.

(b) The traffic phase ''synchronized flow'' possesses a characteristic feature to form diverse spatial-temporal patterns upstream of a highway bottleneck. The downstream

*Electronic address: boris.kerner@daimlerchrysler.com

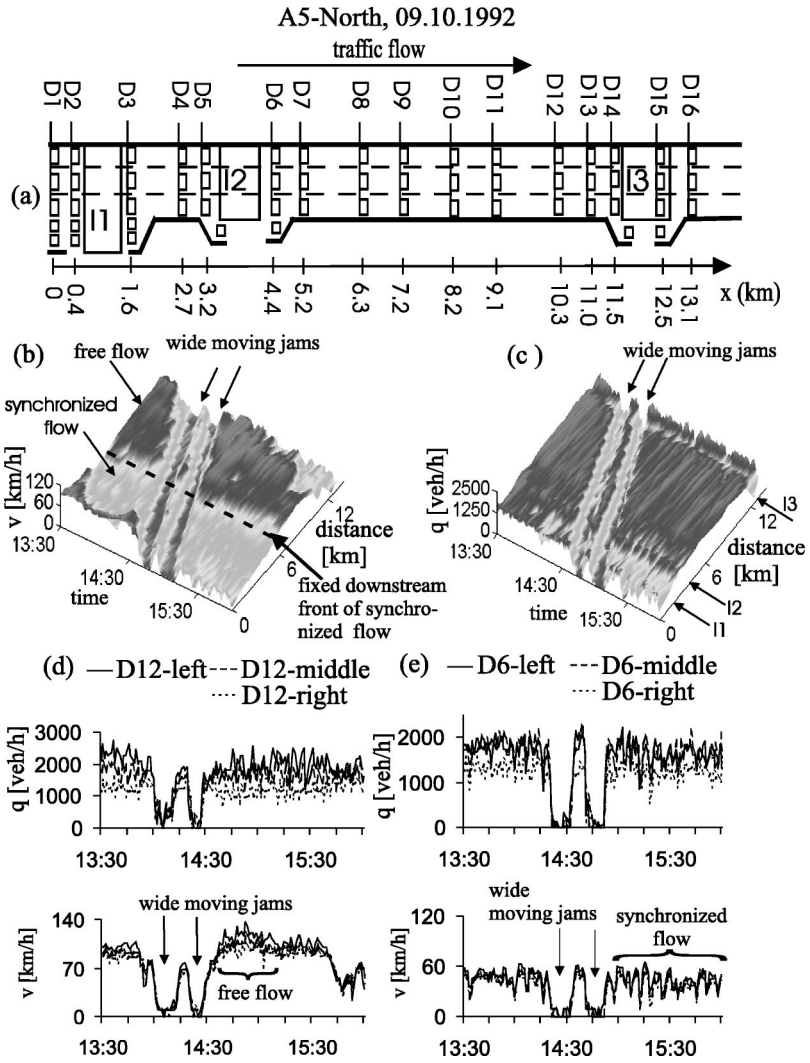

FIG. 1. Explanation of the three traffic phases. (a) A simplified scheme of the infrastructure of the section of the highway A5-North before 1995. The vehicle speed averaged per all highway lanes (b) and the flow rate averaged over the highway (per lane) (c) as functions of time and space on 9 October 1992. Flow rate and the average vehicle speed at $D12$ (d) and $D6$ (e).

front of synchronized flow is usually fixed at the bottleneck. Even if a moving synchronized flow pattern occurs, the velocity of the downstream front of this pattern is not a characteristic parameter. This velocity can change in a wide range during the pattern propagation and it can be different for different patterns.

Besides these features, the traffic phase synchronized flow can show the following other characteristic features.

(i) *The complex transitions effect*. In contrast to free flow, the whole multitude of states of synchronized flow covers a two-dimensional region in the flow-density plane where complex transitions between these different states can occur. In particular, an increase in the vehicle density can be accompanied by both a decrease and an increase in the vehicle speed [56,66].

(ii) *The pinch effect*. A spontaneous self-compression of synchronized flow, i.e., a large increase in the vehicle density at sufficiently high flow rate in synchronized flow [66] (see Sec. III B).

(iii) *The moving jam emergence effect*. A sponteneous occurrence of moving jams in synchronized flow [66] (see Sec. III C).

(iv) *The speed correlation effect*. In synchronized flow, the autocorrelation of the vehicle speed in single vehicle data is large on short scales [61] (see Fig. 15 in Ref. [61]).

(v) *The catch effect*. When synchronized flow that has initially occurred downstream of a bottleneck propagates upstream and reaches the bottleneck, the synchronized flow pattern can be ''caught'' at the bottleneck rather than this pattern propagating further upstream (see Sec. II B 3).

Traffic flow consists of free flow and congested traffic. Congested traffic consists of the phase synchronized flow and the phase ''wide moving jam.'' Thus, there are three traffic phases [56,57,66]: (1) free flow, (2) synchronized flow, (3) wide moving jam.

An example of the application of the criteria for the distinction of wide moving jams from the traffic phase synchronized flow is shown in Fig. 1. The sequence of two moving jams propagates through at least three bottlenecks [in the intersections $I1$, $I2$, and $I3$, Fig. 1(a)] and through different states of synchronized flow [Fig. 1(e), bottom] keeping the velocity of their downstream fronts [70]. Therefore, each of these moving jams belongs to the traffic phase ''wide moving jam.'' In contrast to the wide moving jams, after a congested pattern has occurred upstream of the on ramp at the detectors $D7$, the downstream front of the pattern is *fixed* at the on ramp [see Fig. 1(b), where the downstream front of the pattern is shown by the dashed line]. This pattern belongs

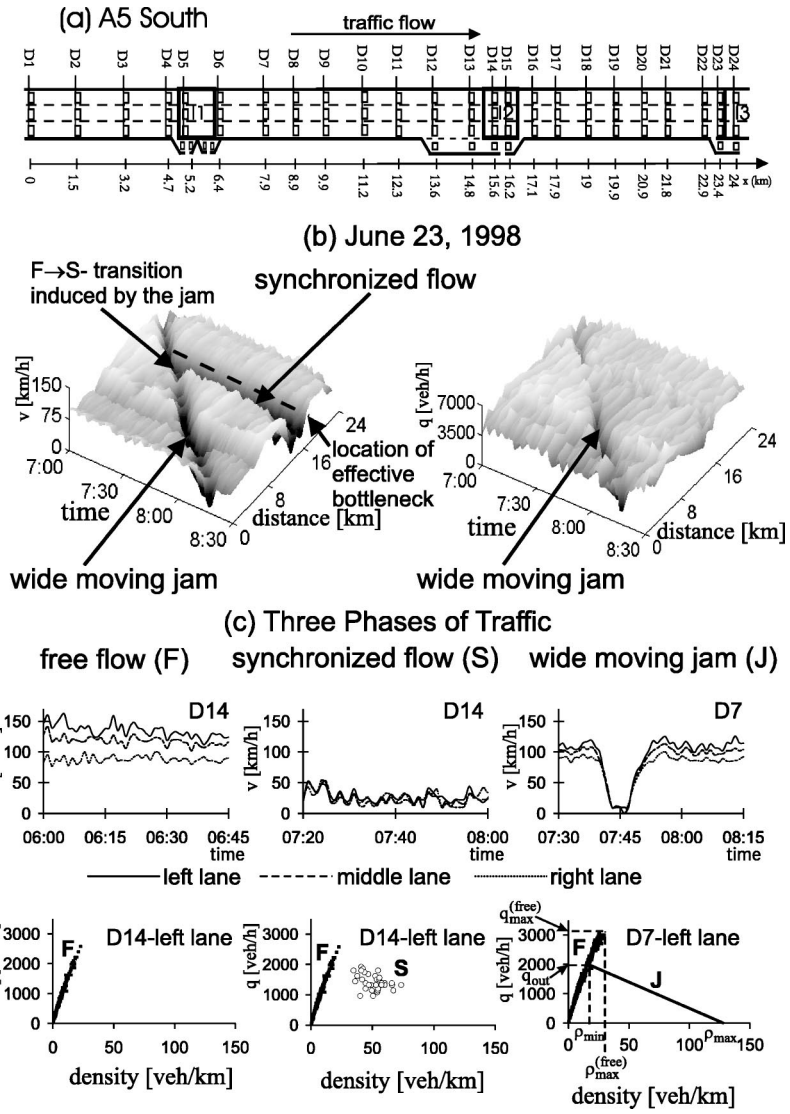

FIG. 2. Explanation of the differentiation between the traffic phases ''wide moving jam'' and ''synchronized flow.'' (a) A simplified scheme of the infrastructure of the section of the highway A5-South. (b) The vehicle speed averaged per all highway lanes (left) and the total flow rate across the highway (right) as functions of time and space measured at the detectors $D1$-$D21$. (c) Top: the average vehicle speed as function of time for free flow (left), for synchronized flow (middle), and for the wide moving jam (right); bottom: the representation of the related traffic phases on the flow-density plane (F is free flow, S is synchronized flow, and the line J is the characteristic line for the downstream front of the wide moving jam). The slope of the line J equals the velocity of the downstream front of the wide moving jam v_g. Traffic data from 23 June 1998.

to the traffic phase synchronized flow.

A different example is shown in Fig. 2 [67–69]. A moving jam propagates through states of free flow (e.g., $D9$–$D12$) and through several bottlenecks inside the three intersections $I1$, $I2$, and $I3$ on a section of the highway A5-South keeping the velocity of the jam's downstream front [this velocity equals the slope of the line J in Fig. 2(c), right]. Therefore, this moving jam belongs to the traffic phase wide moving jam. The wide moving jam propagation through a bottleneck at $D16$ (the on ramp) causes the occurrence of a congested pattern that exists further for a long time upstream of the bottleneck. In contrast to the wide moving jam, the downstream front of this spatial-temporal congested pattern is fixed at the on ramp [in Fig. 2(b) (left) the downstream front of the pattern is shown by the dashed line]. This pattern belongs to the traffic phase synchronized flow. After a study of spatial-temporal features of traffic has been performed and the traffic phases have been distinguished, some features of the found traffic phases may be represented in the flow-density plane [Fig. 2(c)] [62,63].

Possible ways of a theoretical description of the empirical features of the traffic phases synchronized flow and wide moving jam [56–58,62–64,66–68,70] is up to now in a discussion between different scientific groups (e.g., Refs. [36–44,47–50,52,61,74–76]).

A huge number of observations show that patterns of congested traffic as a rule are formed at highway bottlenecks (see books by Daganzo [10] and May [28] and the recent review by Helbing [52]). However, the *empirical* spatial-temporal features of congested patterns that occur at highway bottlenecks still have not been understood sufficiently up to now.

In this paper, results of an empirical study of macroscopic features of spatial-temporal traffic patterns at highway bottlenecks are presented. It will be shown that there are two main types of congested patterns at an isolated bottleneck (the effective bottleneck that is far enough from other effective bottlenecks).

(i) *The general pattern* (GP). GP is the congested pattern at an isolated bottleneck where synchronized flow occurs upstream of the bottleneck and wide moving jams spontaneously emerge in that synchronized flow. Thus GP consists of both traffic phases in congested traffic: synchronized flow and wide moving jam.

(ii) *The synchronized flow pattern* (SP). SP consists of synchronized flow upstream of the isolated bottleneck *only*, i.e., *no* wide moving jams emerge in that synchronized flow. However, dependent on the bottleneck features and on traffic demand, GP and SP show a diverse variety of special cases whose consideration will be one of the main aims of this paper.

The paper is organized as follows. First, empirical features of the phase transition from free flow to synchronized flow (it will be called the $F \rightarrow S$ transition) at on and off ramps will be studied in Sec. II. In Sec. III, GP at on ramps are investigated. It will be shown that the spatial-temporal structure of GP possesses some common predictable, i.e., characteristic, unique, and reproducible features. In Sec. IV an evolution of GP at the on ramp is studied. This evolution occurs when the flow rate to the on ramp gradually decreases over time. It is shown that due to this evolution one type of the congested pattern can transform into another one. Congested patterns that occur at off ramps are considered in Sec. V. Section VI is devoted to a consideration of sometimes very complex congested patterns which can occur when two or more bottlenecks exist close to one another. In the discussion (Sec. VII), a classification of congested patterns, other conclusions of empirical results as well as their qualitatively explanations are made.

II. PHASE TRANSITION FROM FREE FLOW TO SYNCHRONIZED FLOW

A. Representative data sets: Effective bottlenecks

Between 1995 and 2001 different congested patterns on German highways A1, A3, A5, and A44 have been studied. Since it has been found out that the features of these patterns are similar in all cases, some common results may be illustrated by representative data sets presented below that have been measured on the sections of the highway A5-South and A5-North (Fig. 3) (more than 220 congested patterns have been observed on these sections during 1995–2001).

The section of the highway A5-South [Fig. 3(a)] has three intersections with other highways ($I1$, ''Friedberg,'' $I2$, ''Bad Homburger Kreuz,'' and $I3$, ''Nordwestkreuz Frankfurt'') where on and off ramps are located, which may be considered as potential bottlenecks. This section is equipped with 24 sets of induction loop detectors ($D1, \ldots, D24$) [Fig. 3(a)]. Each of the sets $D4$–$D6$, $D12$–$D15$, and $D23$, $D24$ consist of three detectors for a left (passing lane), a middle, and a right lane, plus detectors for the lanes related to on ramps or to off ramps [the detectors on on and off ramps will be designated as $D4$-off, $D5$-on, $\ldots$, $D24$-off-2, see Fig. 3(a)]. The other sets of detectors are situated on the three-lane road without on and off ramps, where each of them consist of three detectors only.

The section of the highway A5-North has four intersections with other highways ($I1$, ''Westkreuz Frankfurt;'' $I2$ ''Nordwestkreuz Frankfurt;'' $I3$, ''Bad Homburger Kreuz;'' and I4, ''Friedberg''). This section is equipped with 30 sets of induction loop detectors ($D1, \ldots, D30$) [Fig. 3(c)] whose designation is the same as for the section of A5-South.

Each detector is a double induction loop detector. This allows to record the crossing of a vehicle and measure its crossing speed. The road computer calculates the flow rate and the average vehicle speed in one minute intervals. Data about vehicle types and individual vehicle speeds of all vehicles passing the detector during each one minute interval are also available.

The overview of some of the representative data are shown in Fig. 3(b) for data measured on A5-South and Fig. 3(d) for data measured on A5-North.

1. Effective bottlenecks on the section on highway A5-South

It has been found that when congested patterns occur on this section, the downstream fronts of these patterns, i.e., the boundaries that separate synchronized flow upstream and free flow downstream are fixed at some locations that are marked as ''B_1,'' ''B_2,'' and ''B_3'' in Fig. 3(b). These locations are the same for all congested patterns that have been observed on the section on A5-South. The locations ''B_1,'' ''B_2,'' and ''B_3'' are therefore related to so called *effective locations* of the bottlenecks on the section on A5-South [Fig. 3(a)]. ''The effective location'' of a bottleneck (or ''the effective bottleneck'' for short) is the location on a highway, which possesses the following two empirical features [67].

(i) The $F \rightarrow S$ transition occurs considerably more frequently at the effective bottleneck in comparison with all other locations on the highway.

(ii) After the occurrence of the $F \rightarrow S$ transition, synchronized flow occurs upstream of the effective bottleneck. The downstream front of synchronized flow is usually fixed at the effective bottleneck.

The effective bottleneck ''B_1'' is linked to the off ramp $D23$-off ($x \approx 23.4$ km). The effective bottleneck ''B_2'' is linked to the on ramp $D15$-on, which is about 100 m upstream of $D16$ ($x \approx 17.1$ km). The effective bottleneck ''B_3'' is linked to the on ramps $D6$-on and $D5$-on about 100 m upstream of $D6$ ($x \approx 6.4$ km).

2. Effective bottlenecks on the section on highway A5-North

The traffic observations on the section on A5-North [Fig. 3(c)] have shown that there are at least three effective bottlenecks there. The first one marked ''$B_{North\,1}$'' [Fig. 3(d)] is linked to the off ramp $D25$-off ($x \approx 22.4$ km), the second one marked ''$B_{North\,2}$'' is linked to the on ramp $D15$-on, which is about 100 m upstream of $D16$ ($x \approx 13$ km), and the third one marked ''$B_{North\,3}$'' is linked to the on ramp upstream of $D6$ ($x \approx 4.4$ km). The features of $F \rightarrow S$ transitions that initially occur at the off ramp $D25$-off and the on ramps ($D16$ and $D6$) are qualitatively similar to those observed at the effective bottlenecks at the off ramp $D23$-off (''B_1'') and the on ramps at $D16$ (''B_2'') and $D6$ (''B_3'') in the section of the highway A5-South [Fig. 3(a)], respectively.

It should be noted that there are also nonhomogeneities on a highway, which do not act as an effective bottleneck, i.e., there the $F \rightarrow S$ transition does not occur. For example, while the off ramp at $D23$-off is often an effective bottleneck on the section of the highway A5-South [Fig. 3(a)], the off ramps at $D5$-off and $D13$-off on this section do not act as an

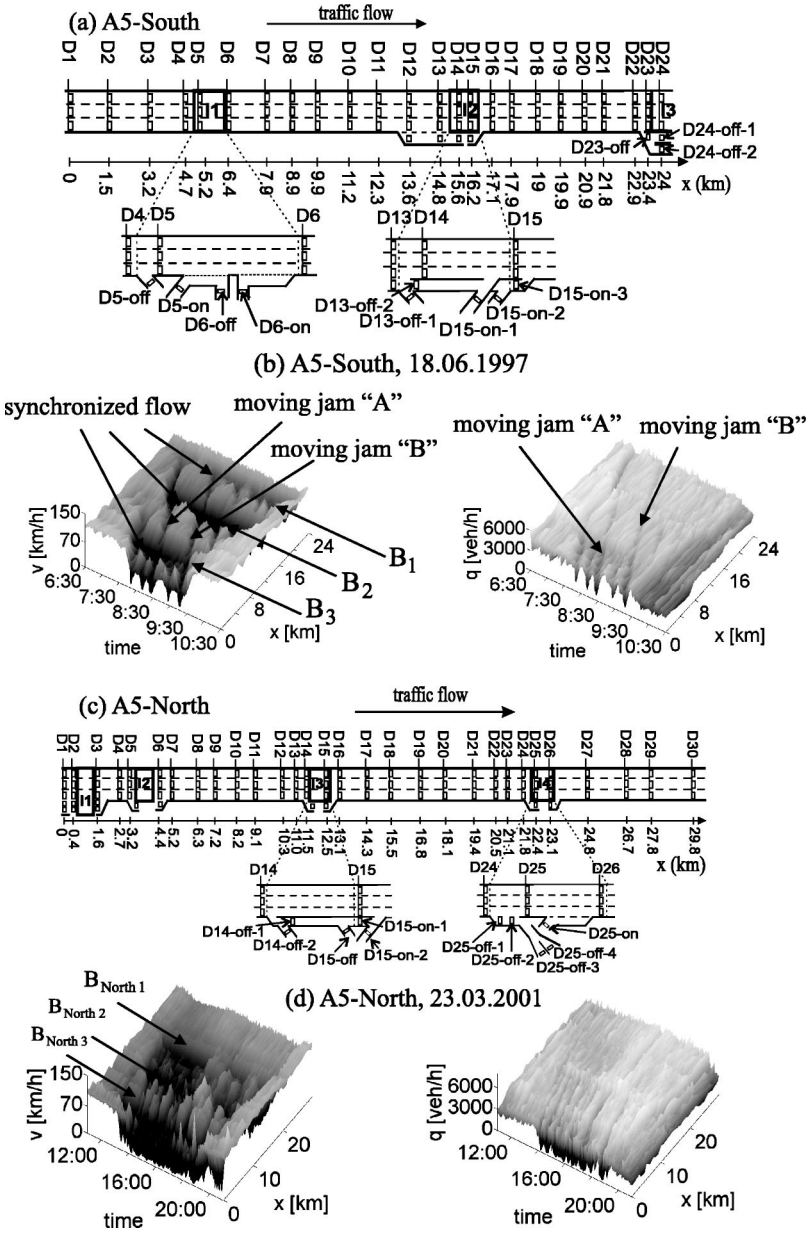

FIG. 3. Representative data sets on the highway A5 in Germany. A scheme of the arrangement of the detectors on the sections of the highway A5-South (a) and one of the related representative data sets (b). A scheme of the highway A5-North in Germany (c) and one of the related representative data sets (d). (b, d) Dependencies of the average (across all lanes) vehicle speed (left) and the total flow rate across the highway (right) on time and space.

effective bottleneck. Indeed, a bottleneck can act as an effective bottleneck if in addition some flow rates that are linked to the particular traffic demand are realized in the vicinity of the bottleneck.

In contrast to the congested patterns in Fig. 3(b), from Fig. 3(d) one might have a first impression that the latter congested pattern would be related to different congested states rather than to a coexistence and to an interaction of two traffic phases in congested traffic, synchronized flow, and wide moving jams. Indeed, it seems that there is no possibility to distinguish wide moving jams in Fig. 3(d). However, this first impression turns out to be incorrect if a more detailed analysis is made (see Sec. V).

B. The $F \rightarrow S$ transition at on ramps

The $F \rightarrow S$ transition at an on ramp and the further effect of the self-maintaining of synchronized flow at the on ramp have already been considered in Ref. [58]. These results have disclosed the nature of the well-known breakdown phenomenon at a highway bottleneck (e.g., Refs. [59,60]). In particular, it has been found that the $F \rightarrow S$ transition is the local first order phase transition [58]. This means that there is a range of high density in free flow where a free flow is in a metastable state. In the metastable state, the *spontaneous* $F \rightarrow S$ transition can occur due to the spontaneous appearance of the local perturbation whose amplitude exceeds some critical amplitude (the nucleation effect).

From the theory and experimental studies of the local first order phase transitions in nonequilibrium distributed (active) physical systems (e.g., Refs. [77,78]) it is well known that in a lot of cases the *induced* phase transition occurs rather than the spontaneous phase transition is realized. In particular, the phase transition in a physical distributed system can be induced by the propagation of a spatial-temporal pattern through the system (e.g., Ref. [78]). The induced $F \rightarrow S$ tran-

sition can also occur in traffic flow at a bottleneck if the flow rates are high enough for the occurrence of the $F \rightarrow S$ transition in free flow. The $F \rightarrow S$ transition can be induced when a wide moving jam propagates through the bottleneck or when a local region of synchronized flow that has initially occurred downstream of the bottleneck reaches the effective location of the bottleneck.

1. The spontaneous $F \rightarrow S$ transition

First, free flow exists both at the on ramp ($D6$) and upstream ($D5$) and also downstream ($D7$) of the on ramp [$t < 06{:}37$ in Figs. 4(a,b)]. At $t \approx 06{:}37$ a sudden fall (the ''breakdown'') in the average vehicle speed at $D6$ occurs [see up arrow at $D6$, Fig. 4(b), left and the related arrow in Fig. 4(c)]. The speed at $D6$ becomes considerably lower than the minimum vehicle speed at the limit point for free flow $\rho_{max}^{(free)}, q_{max}^{(free)}$. During the transition at $D6$ the free flow conditions exist both upstream ($D5$) and downstream ($D7$). The downstream front of the pattern that is developing after this transition has occurred is fixed at the on ramp [Fig. 4(a)]. Thus, this transition is the spontaneous $F \rightarrow S$ transition at the on ramp.

After the $F \rightarrow S$ transition at $D6$ has occurred, the average vehicle speed in synchronized flow shows only relatively small changes of about 10% over time near 65 km/h at $D6$ [Fig. 4(b)]. The same behavior of the speed in synchronized flow is observed on all other days at $D6$.

It must be noted that the $F \rightarrow S$ transition leads to the further self-maintaining of synchronized flow at the on ramp during about 2.5 h on 17 March 1997. However, there are a lot of cases when the $F \rightarrow S$ transition at the on ramp does not lead to the effect of the self-maintaining of synchronized flow: the synchronized flow exists only during a short time at the on ramp. Such cases are shown in Fig. 4(d) (the up arrows 1, 2, and 3, $D6$) where for a comparison the $F \rightarrow S$ transition at $t \approx 06{:}37$ (marked by the up arrow 4) considered above [Fig. 4(a–c)] is shown.

To understand this different behavior, recall that the vehicle speed in synchronized flow is always lower than the minimum vehicle speed in free flow. Therefore, correspondingly to the vehicle balance equation [1,17], after a local region of synchronized flow has occurred at the on ramp, the upstream front of this synchronized flow can propagate upstream only if the average flow rate in free flow upstream is higher than the average flow rate in the synchronized flow. A comparison of the flow rates over the whole highway at $D6$, q_{D6} [solid curve ''$D6$'' in Fig. 4(e)] with the sum of the flow rates, q_{sum} (dashed curve) upstream of $D6$ for these different $F \rightarrow S$ transitions is made in Table I. Here $q_{sum} = q_{D5} + q_{D6\text{-}on} + q_{D5\text{-}on} - q_{D6\text{-}off}$, where q_{D5}, $q_{D6\text{-}on}$, $q_{D5\text{-}on}$, and $q_{D6\text{-}off}$ are the flow rates at $D5$, at the on ramp $D6$-on, at the on ramp $D5$-on, and at the off ramp $D6$-off.

In the cases 1, 2, and 3, $q_{sum} < q_{D6}$ (Table I). This explains why the upstream front of the synchronized flow at the on ramp ($D6$) does not propagate upstream. In contrast, for the $F \rightarrow S$ transition, which is marked by the up arrows 4 in Figs. 4(d) and 4(e) $q_{sum} > q_{D6}$ (Table I). As a result, the upstream front of the synchronized flow propagates upstream

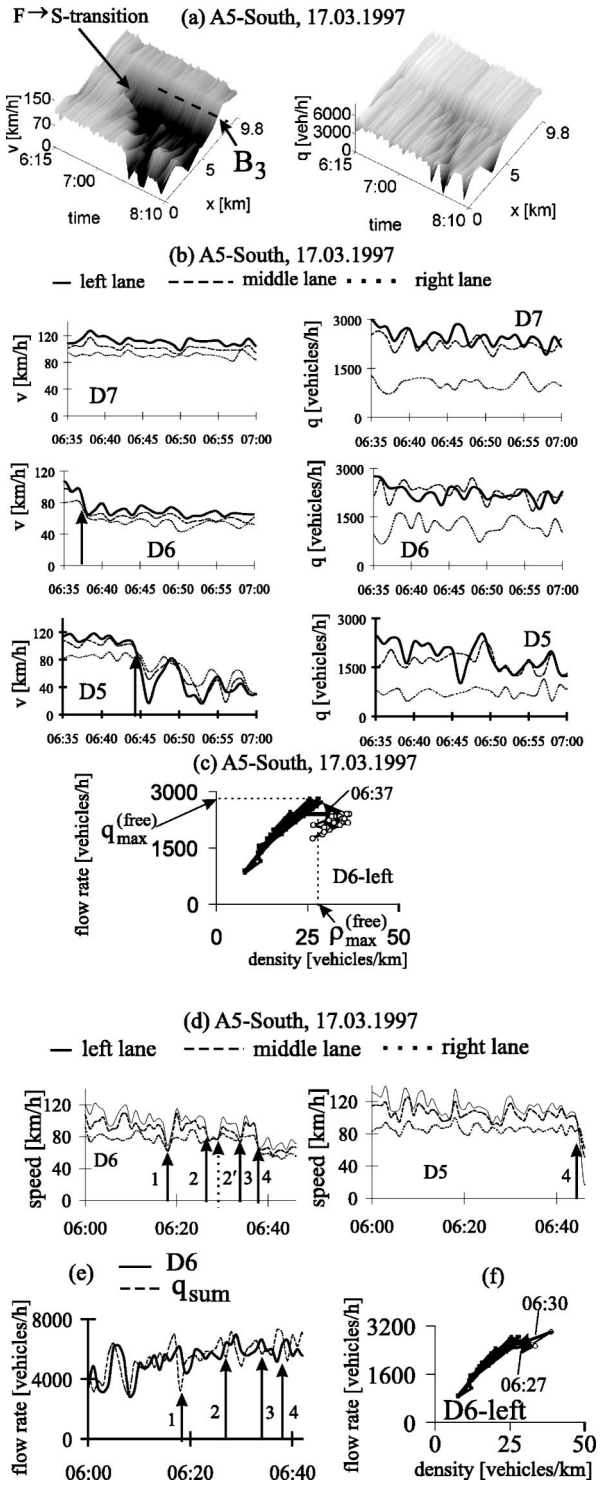

FIG. 4. The $F \rightarrow S$ transition at the on ramp ($D6$) on 17 March 1997. (a) The overview of the vehicle speed averaged over all highway lanes (left) and the total flow rate across the highway (right), (b) the vehicle speed (left) and the flow rate (right) at different detectors, (c) the $F \rightarrow S$ transition in the flow-density plane. (d–f) A comparison of different $F \rightarrow S$ transitions at the on ramp: (d) the vehicle speed at $D6$ and $D5$, (e) the flow rates at $D6$ and upstream of $D6$ (q_{sum}), (f) the $F \rightarrow S$ transition in the flow-density plane, which does not lead to the pattern formation [arrows at 6:27 and at 6:30 are related to the up arrows 2 and 2′ in (d) (left), respectively].

TABLE I. The average flow rates during the $F \rightarrow S$ transitions. In the second column, the time intervals are given where the flow rate after the related $F \rightarrow S$ transition has occurred has been averaged. These intervals are chosen to be higher than the trip time of vehicles between $D5$ and $D6$ (the latter is less than 3 min).

$F \rightarrow S$ transition	Interval	q_{D6} (vehicles/h)	q_{sum} (vehicles/h)
Arrow 1 ($t=6{:}18$)	6:18–6:21	5080	4580
Arrow 2 ($t=6{:}27$)	6:27–6:31	6230	5850
Arrow 3 ($t=6{:}34$)	6:34–6:37	6180	5780
Arrow 4 ($t=6{:}37$)	6:37–6:40	6020	6520

and reaches the location of $D5$ [the up arrow 4 on Fig. 4(d), $D5$]. In this case, the self-maintaining of the synchronized flow at the on ramp indeed occurs.

2. The induced F→S transition caused by a moving jam propagation through an effective bottleneck

An example of the $F \rightarrow S$ transition at the on ramp induced by a moving jam propagation through the bottleneck B_2 at the on ramp ($D16$) on the highway A5-South is shown in Figs. 2(b), left and Fig. 5. First, it should be noted that during the whole time before the moving jam reaches the on ramp, free flow is realized both at $D16$ and upstream ($D15$) and also downstream ($D17$) [Fig. 5(a)]. However, after the moving jam has passed the on ramp a synchronized flow is formed at the on ramp. (i) This synchronized flow exists further for a long time at the bottleneck and (ii) the downstream front of the synchronized flow is fixed at the bottleneck. Thus, the $F \rightarrow S$ transition is induced at the on ramp during the jam propagation.

It may be assumed that after the moving jam has just passed the on ramp the still slow moving vehicles that are escaping from the moving jam force the vehicles at the on ramp to move slow too. This may cause this $F \rightarrow S$ transition.

3. The induced F→S transition caused by a propagation of synchronized flow. The catch effect

SP has occurred at the bottleneck B_1 (the off ramp, $D23$-off) in Fig. 6(a), left. Both the upstream and downstream fronts of this SP are moving upstream, i.e., the moving SP (MSP) occurs (see also Secs. II C and V B). When the upstream front of MSP reaches the bottleneck B_2 at the on ramp ($D16$) another SP that is further localized at the bottleneck B_2 is formed. The downstream front of this localized SP (LSP) is fixed at the on ramp [Fig. 6(a), left] and this LSP is further self-maintained from 06:49 to 09:25. Thus, the upstream propagation of the initial MSP indeed induces the $F \rightarrow S$ transition at the on ramp.

In contrast to the case when a wide moving jam propagates through the bottleneck B_2 keeping the jam's downstream front velocity [Figs. 2(b) and Fig. 5, the down arrows], MSP *is caught* at the on ramp (*the catch effect*).

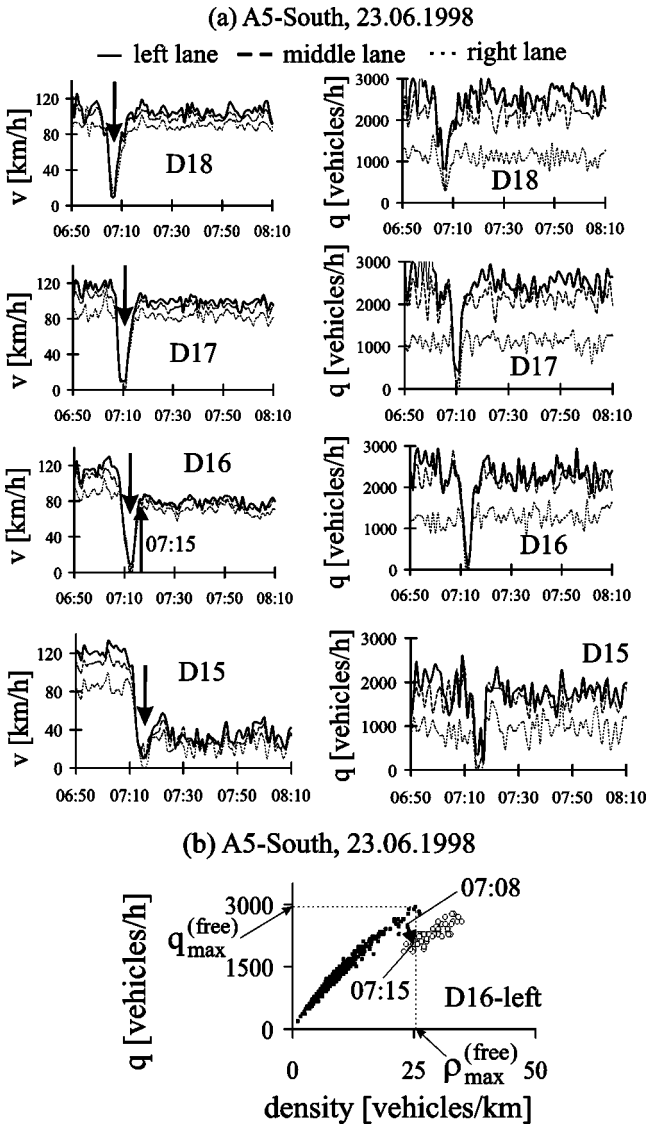

FIG. 5. The $F \rightarrow S$ transition at the on ramp ($D16$) caused by the moving jam propagation on 23 June 1998 [see the overview in Fig. 2(b), left]. (a) The vehicle speed (left) and the flow rate (right) at different detectors, (b) the $F \rightarrow S$ transition in the flow-density plane.

Indeed, after MSP has reached the bottleneck a qualitatively different LSP occurs there. This LSP is determined most by the characteristic of the bottleneck, traffic demand, and highway peculiarities upstream (see also Sec. VI C). There is also another difference between a wide moving jam and MSP. In contrast to the wide moving jam, inside MSP the vehicle speed is higher than in the jam [about 40–70 km/h, Fig. 5(b)] and the average flow rate is only a little bit lower than in the initial free flow.

In another example, after a local region of synchronized flow ($D7$), which has initially occurred between the bottlenecks B_2 and B_3 has reached the bottleneck B_3 ($D6$), synchronized flow occurs upstream of this bottleneck ($D5$). This synchronized flow is further self-maintained during 2.3 h. Thus, the upstream propagation of the synchronized flow also induces the $F \rightarrow S$ transition at the on ramp ($D6$).

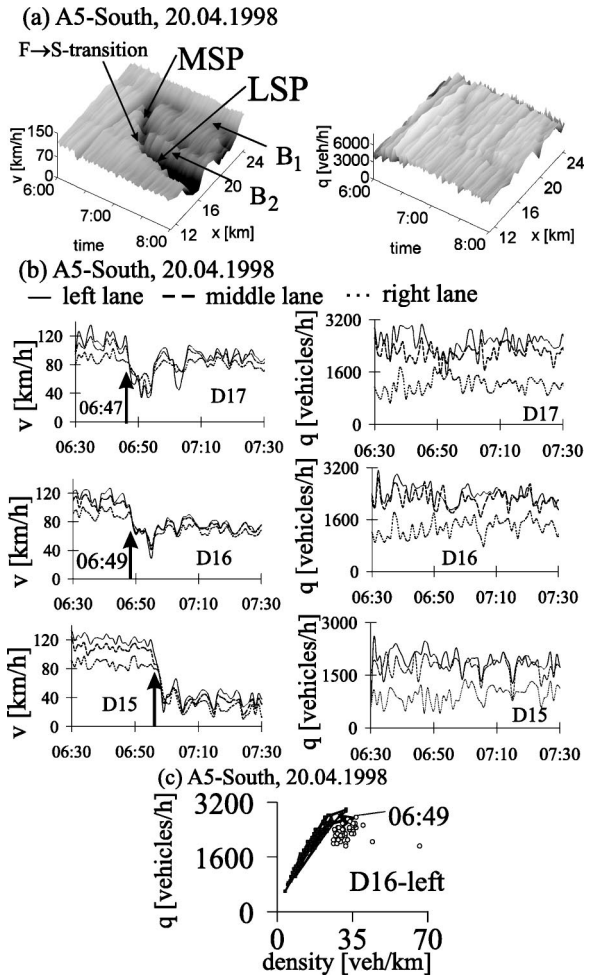

FIG. 6. The $F\rightarrow S$ transition at the on ramp ($D16$) caused by the propagation of the moving synchronized flow pattern on 4 April 1998. (a) The overview of the averaged vehicle speed over the highway (left) and the total flow rate across the highway (right), (b) the vehicle speed (left) and the flow rate (right) at different detectors, (c) the $F\rightarrow S$ transition in the flow-density plane. MSP is the moving synchronized flow pattern, LSP is the localized synchronized flow pattern.

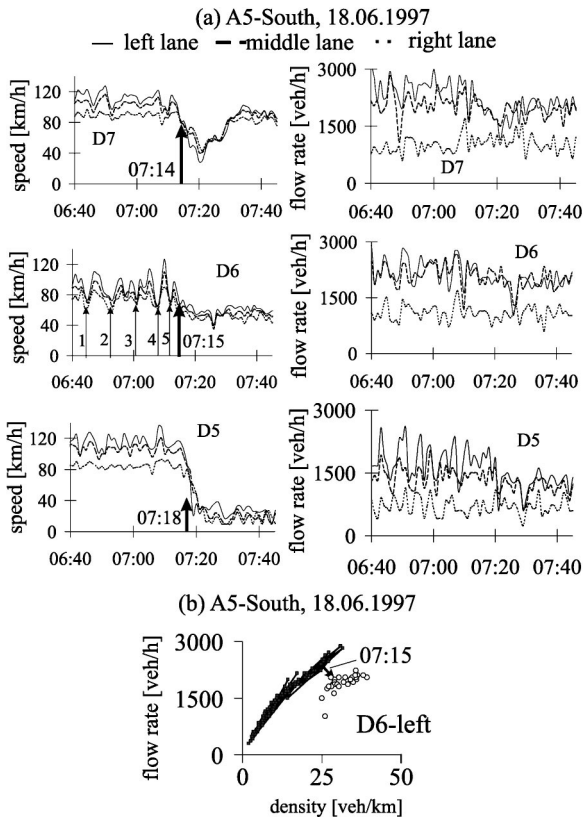

FIG. 7. The $F\rightarrow S$ transition at the on ramp ($D6$) caused by the propagation of a local region of synchronized flow on 18 June 1997. (a) The vehicle speed (left) and the flow rate (right) at different detectors, (b) the $F\rightarrow S$ transition in the flow-density plane.

Note that before the latter induced $F\rightarrow S$ transition occurs, at least four spontaneous $F\rightarrow S$ transitions are observed at the on ramp, which do not lead to the effect of the self-maintaining of the synchronized flow at the on ramp (the up arrows 1–5 in Fig. 7). The latter cases are similar to the cases considered above [see Fig. 4(d), the up arrows 1, 2, and 3].

C. The $F\rightarrow S$ transition at off ramps

It is well known that traffic congestion upstream of an off ramp can occur, if the fraction of vehicles that have to choose the off ramp is high enough (see, e.g., Ref. [10]).

An example is shown in Fig. 8 where the ratio of the vehicles moving on the right lane q_{right} to the whole flow rate on the highway q_{whole}, $\delta=q_{right}/q_{whole}$ is a continuously increasing function of the distance from intersection $I2$ to intersection $I3$ [Fig. 8(b)]. As a result, the flow rate of the vehicles that move on the right lane is drastically increasing from $D21$ (21.8 km) to $D22$ (22.9 km).

Apparently the latter effect causes the fall of the speed on the right lane at $D22$ [up arrow at $D22$, Fig. 8(a)]. Most of the vehicles that move on the middle and the left lane at $D22$ have a different route in comparison to those vehicles that want to leave to the off ramp. This may be the reason why the synchronization of the speeds on different highway lanes does not occur at $D22$.

The synchronized flow occurs only at $D21$, i.e., about 1.5 km upstream of the off ramp. The reason for this synchronized flow and of the related $F\rightarrow S$ transition is the fall in the vehicle speed at the bottleneck B_1 due to the off ramp. Between $D21$ and $D22$ a lot of vehicles change to the right lane [Fig. 8(b)], where the speed is lower. These vehicles may force the vehicles on the middle and left lane, which want to continue on the highway, to slow down.

Note that due to this $F\rightarrow S$ transition at the off ramp the MSP [Fig. 6(a), left and Fig. 8(a), $D21$, $D20$] occurs whose upstream propagation causes later the induced $F\rightarrow S$ transition at the upstream bottleneck B_2 considered above (see Sec. II B 3).

Therefore, in comparison with the $F\rightarrow S$ transitions at on ramps, in the case of an off ramp synchronized flow occurs at some distance upstream of the off ramp. It may be proposed that the effective location of the bottleneck due to the off

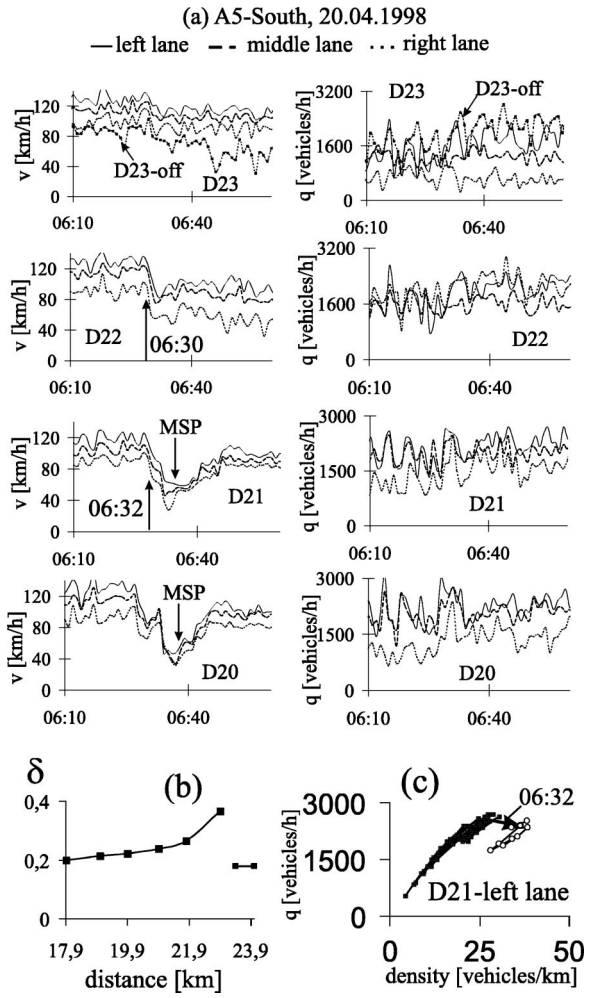

FIG. 8. The $F\rightarrow S$ transition at the off ramp $D23$-off on 20 April 1998. (a) The vehicle speed (left) and the flow rate (right) at different detectors, (b) the ratio $\delta=q_{right}/q_{whole}$ as the function of the distance, (c) the $F\rightarrow S$ transition in the flow-density plane. The down arrows ''MSP'' at $D22$ and $D21$ in (a) (left) are related to the vehicle speed distribution in the moving synchronized flow pattern (MSP) whose overview is shown in Fig. 6(a), left.

ramp is also located at some distance upstream from the off ramp.

However, both at on and off ramps the $F\rightarrow S$ transition is accompanied by the fall in the vehicle speed [the arrows in Figs. 4(c), 5(b), 6(c), 7(b), and 8(c)] whose duration is not higher than about 1 min. Besides, although the speed decreases noticeably during the $F\rightarrow S$ transition (the ''breakdown''), the flow rate in the emerged synchronized flow can remain of the same order of magnitude as in the initial free flow.

III. PREDICTABLE FEATURES OF GENERAL PATTERNS AT ON RAMPS

A. The general pattern at isolated effective bottlenecks

1. Isolated bottleneck

Here we restrict to the consideration of features of GP at such an effective bottleneck that is located far enough from other bottlenecks. Exactly the effects of other bottlenecks and/or any other nonhomogeneities on the highway away from the effective bottleneck should not have a qualitative influence on the features of the pattern at the effective bottleneck. Such an effective bottleneck will be called an *isolated* effective bottleneck (an isolated bottleneck for short).

Inside the intersection $I1$ on the highway A5-South there are several on ramps or/and off ramps. However, the $F\rightarrow S$ transition and congested patterns are observed *always only* at the same location in the vicinity of $D6$ [Fig. 3(a)] (about 110 congested patterns upstream of $D6$ have been observed). Other possible effective bottlenecks are located on the road far enough from $D6$.

However, in this case, there are two on ramps, $D5$-on and $D6$-on, which are very close to one another [Fig. 3(a)]. The end of the on ramp $D6$-on is located about 100 m upstream of $D6$. The length of the on ramp $D6$-on where vehicles may enter the highway section is about 290 m. The end of the other upstream on ramp $D5$-on and the beginning of the on ramp $D6$-on are separated only by about 83 m. The length of the on ramp $D5$-on is 325 m. The latter on ramp is used also as the off ramp $D6$-off for vehicles that leave the highway A5-South. Because the distance between the on ramps $D5$-on and $D6$-on is noticeable shorter then the length of each of the on ramps, they may also be considered as one effective on ramp on this section with the effective flow rate $q_{eff\text{-}on}$:

$$q_{eff\text{-}on}=q_{D6\text{-}on}+q_{D5\text{-}on}-q_{D6\text{-}off}. \tag{1}$$

The congested patterns upstream of $D6$ are fully formed within about 4–5 km upstream (Figs. 9–11). The next upstream intersection, where other effective bottlenecks can exist, is located about 10 km upstream from $D6$. Thus, the effective bottleneck at $D6$ can indeed be considered as an isolated bottleneck at the on ramp. Nevertheless, to demonstrate that the qualitative results below are independent of either (i) the effective flow rate $q_{eff\text{-}on}$ only alone or (ii) the flow rate $q_{D6\text{-}on}$, or else (iii) the flow rate $q_{on\text{-}up}=q_{eff\text{-}on}-q_{D6\text{-}on}$ is responsible for the pattern features, all these flow rates will be studied.

2. Some features of the general pattern

After the $F\rightarrow S$ transition has occurred at $D6$, a congested pattern can be formed upstream of $D6$. Observations show that independent of the initial conditions, i.e., traffic demand (the initial flow rates on the highway, q_{in} and to the effective on ramp, $q_{eff\text{-}on}$), percentages of long vehicles A_{long}, and the weather conditions, in more than 90% cases the congested pattern is GP. This GP has been qualitatively the same as it has earlier been found and investigated in Ref. [66] (Fig. 9).

In a lot of cases two parts may be distinguished in GP [Fig. 9(b)]: (i) The synchronized flow that is upstream bordered by (ii) a sequence of wide moving jams, or the region of wide jams for short.

In the synchronized flow in GP [Fig. 9(b)], the pinch region is formed where narrow moving jams emerge and grow propagating upstream ($D5, D4$). The downstream front

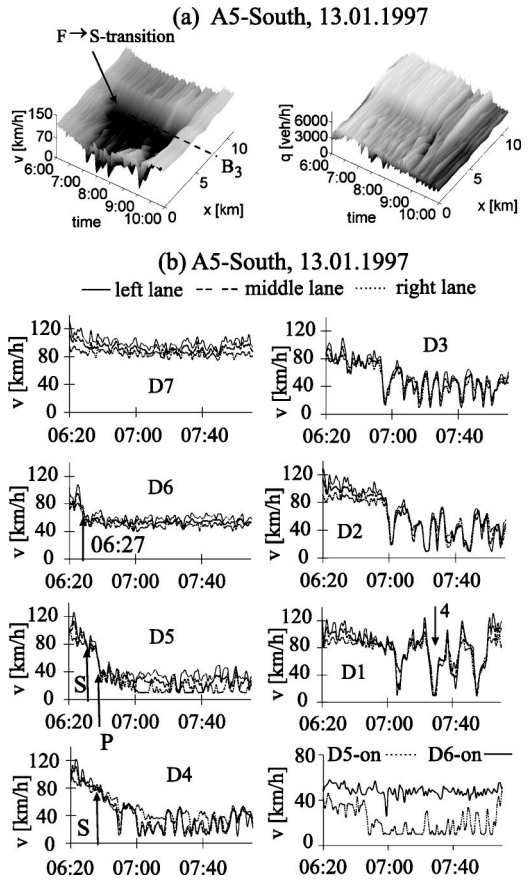

FIG. 9. The general pattern (GP) upstream of $D6$ (the effective bottleneck B_3) on the section of the highway A5-South [Fig. 3(a)] on 13 January 1997. (a) The overview of GP: the vehicle speed averaged over all lanes (left) and the flow rate over the whole highway (right) in space and time; (b) the vehicle speed on different lanes in GP at different detectors.

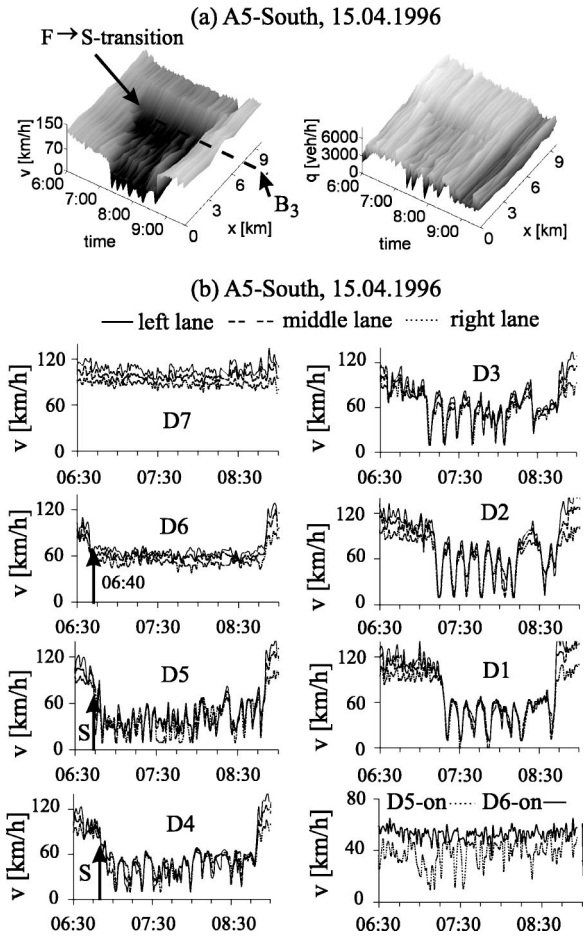

FIG. 10. The general pattern (GP) upstream of $D6$ (the effective bottleneck B_3) on the section of the highway A5-South [Fig. 3(a)] on 15 April 1996. (a) The overview of GP: the vehicle speed averaged over all lanes (left) and the flow rate over the whole highway (right) in space and time; (b) the vehicle speed on different lanes in GP at different detectors.

(boundary) of the synchronized flow is located at the effective location of the bottleneck. The upstream front (boundary) of the synchronized flow is determined by the location where a narrow moving jam is just transformed into a wide moving jam, i.e., where the phase transition from synchronized flow to a wide moving jam (it will be called the $S \rightarrow J$ transition) has occurred. The upstream boundary separates the synchronized flow downstream and the region of wide jams upstream. When a wide moving jam occurs, the jam suppresses the further growth of the narrow moving jams that are very close to the downstream front of this wide moving jam. As a result, some of narrow moving jams can disappear without their transformation into wide moving ones [66]. Because the transformation of different narrow moving jams into wide moving jams can occur at different locations, the upstream boundary of synchronized flow performs complex spatial oscillations over time. The mean width of the synchronized flow in GP, L_{syn}, is limited: $L_{syn} \approx 3-4$ km, i.e., it does not noticeably depend on traffic demand.

The successive process of the transformation of narrow moving jams into wide moving jams at the upstream boundary of synchronized flow leads to the formation of the region of wide moving jams. Due to the upstream wide jam propagation, the region of wide jams is continuously widening upstream. Consequently, the quantity of wide moving jams inside the region of these jams can increase over time. Between wide moving jams both synchronized flow and free flow can be formed. These flows will be considered as a part of the region of wide jams.

3. The general patterns on three different days

Let us compare the features of GP that have emerged at the effective bottleneck at $D6$ on three different days (on three different years). This allows to study common features of GP that have been observed on all other days during 1995–2001. The first general pattern from 13 January 1997 is shown in Fig. 9 (Fig. 1 in Ref. [66]). The second and the third general patterns from 15 April 1996 (Fig. 10) and from 23 March 1998 (Fig. 11) are very similar.

In these three cases, downstream of GP, i.e., at $D7$, free flow conditions are realized (Figs. 9, 10, 11). Therefore, all these congested patterns can be indeed considered as the general pattern at the isolated bottleneck at $D6$. The up ar-

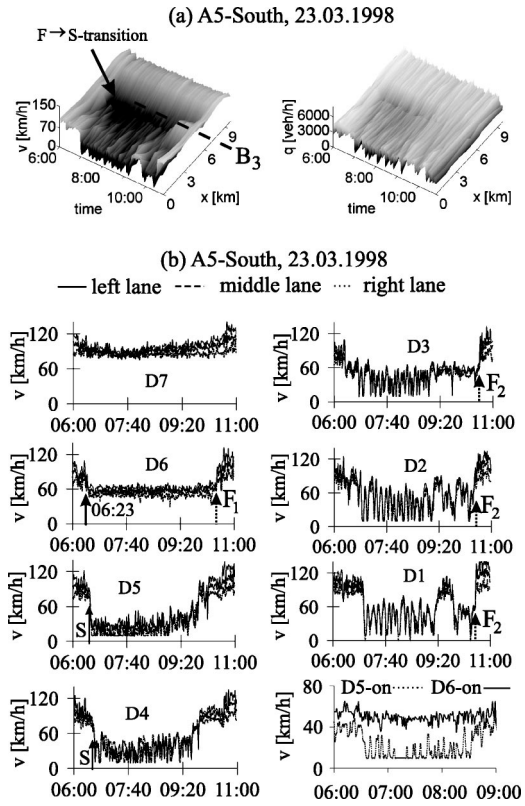

FIG. 11. The general pattern upstream of $D6$ (the effective bottleneck B_3) on the section of the highway A5-South [Fig. 3(a)] on 23 March 1998. (a) The overview of GP: the vehicle speed averaged over all lanes (left) and the flow rate over the whole highway (right) in space and time; (b) the vehicle speed on different lanes in GP at different detectors.

row at $D6$ in Figs. 9(b), 10(b), and 11(b) symbolically shows the time t_{FS} (Table II) when the $F \rightarrow S$ transition at the on ramp occurs leading to the GP formation upstream ($D6$-$D1$).

To compare the initial conditions of the GP formation, the time dependencies of the flow rate to the on ramps $D6$-on, $D5$-on, to the off ramps $D6$-off and $D5$-off, as well as of the flow rate to the effective on ramp, $q_{eff\text{-}on}$ (''eff-on''), which are averaged over 10 min intervals, are shown in Fig. 12 for the three days. The up arrows 1, 2, and 3 in Fig. 12 ($D6$-on and ''eff-on'') are related to the corresponding times t_{FS} (Table II). The time intervals where the congested patterns upstream of $D6$ exist are also marked in Fig. 12 ($D6$ and $D1$).

TABLE II. Parameters for the general patterns formation and evolution on three different days on the section of the highway A5-South

Parameter or characteristic	Day		
	15 April 1996	13 January 1997	23 March 1998
t_{FS}	06:40	06:27	06:23
$q_{eff\text{-}on}$ (vehicles/h)	1680	1440	1500
$t_{eff\text{-}on}$	07:09	07:43	07:10
$q_{eff\text{-}on,\,max}$ (vehicles/h)	1980	1830	1800
$q_{eff\text{-}on}^{(trans)}$ (vehicles/h)	900–600	570–480	780–600

4. Overview of the flow rates in the general pattern

The downstream front of synchronized flow where vehicles accelerate from synchronized flow upstream to free flow downstream is fixed at the effective bottleneck ($D6$). Thus, the flow rate inside this front—the discharge flow rate $q_{out}^{(bottle)}$—does not depend on the space coordinate [60]. However, the discharge flow rate can noticeably depend on time (Fig. 12, $D6$) [67]. It must be noted that whereas the flow rates to on ramps are very similar for the three days, the discharge flow rates ($D6$) are noticeably different.

This is because the average flow rate inside the pinch region, $q^{(pinch)}$ (at $D5$) is also noticeably different for all these days and on the other hand, the sum of $q^{(pinch)}$ and $q_{eff\text{-}on}$ gives approximately the average discharge flow rate at $D6$, $q_{out}^{(bottle)}$:

$$q_{out}^{(bottle)} = q^{(pinch)} + q_{eff\text{-}on}. \tag{2}$$

Let us show that the mentioned differences in the discharge flow rate $q_{out}^{(bottle)}$ ($D6$) and the flow rate inside the pinch region $q^{(pinch)}$ ($D5$) are correlated with the differences in the flow rate in the outflow of a wide moving jam, q_{out}, when in this outflow free flow is formed.

B. Pinch effect and characteristic parameters of wide moving jams

1. Determination of the line J

A wide moving jam possesses the characteristic (i.e., unique, reproducible, and predictable) parameters [70]. These parameters depend only on the control parameters of traffic such as the percentage of long vehicles, infrastructure, weather, and other environmental conditions. One of these parameters is the mean velocity of the downstream front of the wide moving jam, v_g [70]. It is important that this velocity remains the characteristic parameter independent of the states of flow in the outflow of the wide moving jam. The related stationary movement of the downstream front of a wide moving jam can be represented in the flow-density-plane as a line whose slope equals v_g. This characteristic line for the downstream front of the moving jam is called ''the line J'' (Fig. 13) [70].

To determine the line J with empirical data, the following procedure has been used [56,70]. When a wide moving jam passes a detector, the time series of the vehicle speed and the flow rate can be measured. An example is shown in Figs. 13(a, b) for a wide moving jam at $D11$. Similar measurements of the time series of the vehicle speed can be performed at different detectors due to the jam propagation through the highway. Using the distances between the different detectors it is easy to calculate the mean velocity of the

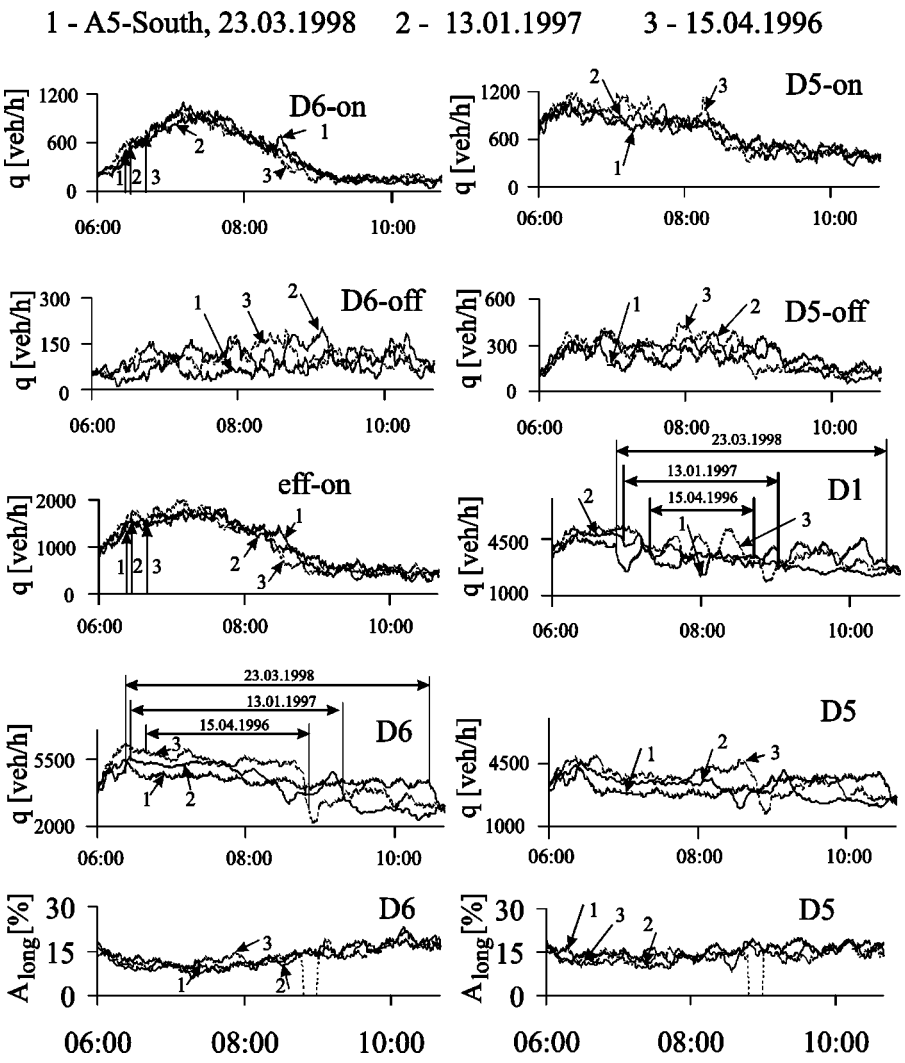

FIG. 12. A comparison of the flow rates and of the percentage of long vehicles A_{long} at different locations related to the congested patterns observed on three different days. 10 min averaged data: each 10 min averaged value is set to the minute at which the 10 min interval of the averaging begins. This interval of the averaging is noticeably higher than the travel time between $D6$ and $D5$, which is less than 3 min.

downstream front of the wide moving jam, v_g, within the accuracy of the measurements (1 min intervals) (Table III).

Besides this mean velocity, the flow rate and the vehicle speed downstream of the wide moving jam can be measured. If in the outflow from the wide moving jam a free flow is formed, then the mean flow rate in this outflow q_{out}, the mean vehicle speed v_{max}, and the related mean density ρ_{min}, are also the characteristic parameters which are the same for different wide moving jams at given control parameters of traffic [70]. The density ρ_{min} can be estimated by the formula $\rho_{min}=q_{out}/v_{max}$ (Fig. 13). These parameters of the wide jam outflow determine the coordinate (q_{out},ρ_{min}) of the boundary point of the line J in the flow-density plane. Thus, from the measurements we find this coordinate and the slope of the line J, which is given by the velocity v_g. This allow us to draw the line J and to estimate the average vehicle density inside the jam ρ_{max} as the intersection point of the line J and the axis of the density (x axis). It should be noted that to avoid the influence of fluctuations, for the determination of the flow rate out from a wide moving jam usually the flow rate during a few minutes interval after the jam has passed the detectors is used. However, during this averaging time interval one should take care that on the one hand only the vehicles that have escaped from the jam are taken into account and on the other hand all of these vehicles are taken into account. In other words, the detectors where the flow rate out from a wide moving jam is measured should be far enough from any on and off ramps. It must also be noted that the line J is related to the downstream jam front only and that only the flow rate in the outflow of the downstream front and the velocity of this front are used for the definition and for the determination of the line J rather than the traffic states of the downstream jam front falling on the line J.

Results of the study of wide moving jams that propagate through the highway section are shown in Fig. 13 and Table III. One of these wide moving jams is shown in Fig. 13(g). In this case, synchronized flow is formed in the outflow of this wide moving jam. However, even in such a case it is possible to estimate with a good accuracy the jam's characteristic parameters. Indeed, if synchronized flow is formed downstream of a wide moving jam, the average flow rate in this flow, $q_{out}^{(syn)}$, is lower than q_{out}. However, the point in the flow-density plane related to the flow rate $q_{out}^{(syn)}$ is close to a point at the line J [Fig. 13(i)]. Therefore, the line J can be approximately found if the flow rate $q_{out}^{(syn)}$ and the speed in the synchronized flow averaged during 5–10 min are taken for

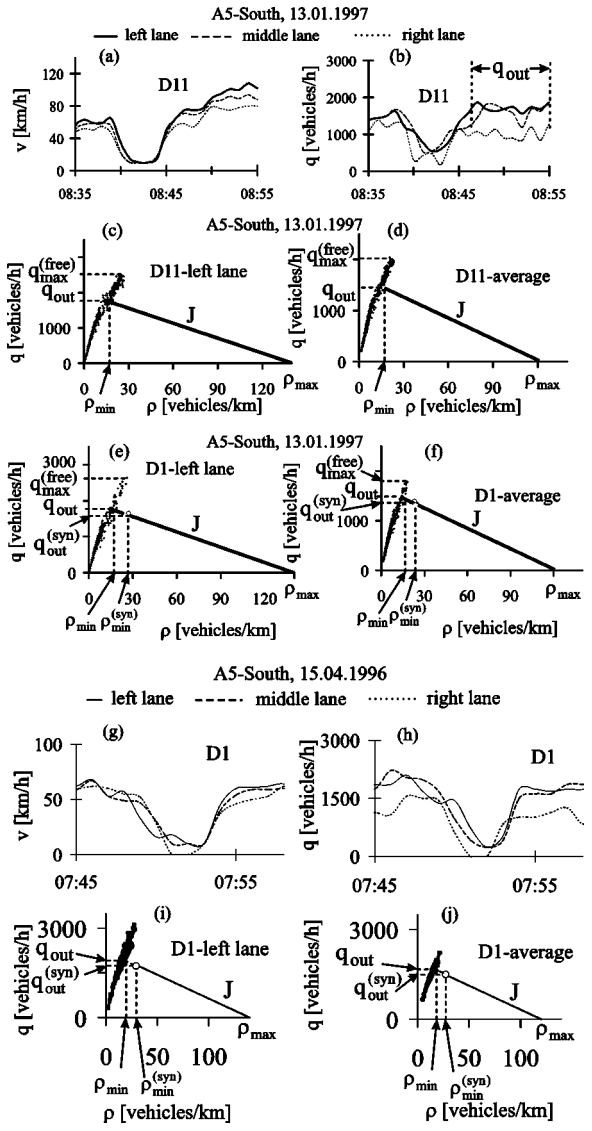

FIG. 13. Determination of the line *J*. (a) The vehicle speed (left) and the flow rate (right) in a wide moving jam at $D11$ on the section of the highway A5-South [Fig. 3(a)] on 13 January 1997; (c–f) free flow (back points) and the line *J* in the flow-density plane for two different wide moving jams: (c, d) for the jam at $D11$, (a, b) and (e, f) for the wide moving jam marked by the arrow 4 in Fig. 9 at $D1$. The vehicle speed (g) and the flow rate (h) in a wide moving jam at $D1$ on the section of the highway A5-South [Fig. 3(a)] on 15 April 1996 (a); (i, j) free flow (back points) and the line *J* in the flow-density plane related to (g, h).

the determination both of the density $\rho_{min}^{(syn)}$ and of the left coordinate of the line *J*. This allows to estimate the flow rate q_{out} as the point where the line J crosses the region of free flow in the flow-density plane [Fig. 13(i)].

To prove the correctness of such a procedure, different wide moving jams have been studied. It has been found that with the accuracy of about 5% (at least three different wide moving jams at each of the three days have been studied) the determination of q_{out} with the above procedure has led to the same result. The analogous result for 13 January 1997 is shown in Fig 13(e, f).

On 13 January 1997 a wide moving jam at $D11$ [Fig. 13(a, b)] has been chosen for comparison with the estimated value of q_{out} for the wide moving jam that is marked by the down arrow 4 (the jam 4 for short) in Fig. 9 at $D1$. In the case of the jam at $D11$ free flow conditions are in the outflow from the jam [Fig. 13(a)]. In the case of the jam 4 in Fig. 9 ($D1$) synchronized flow is formed in the outflow of the jam. However, the measured flow rate q_{out} for the jam at $D11$ [Fig. 13(c,d)] is, with the accuracy within 5%, the same as that estimated for the jam 4 [Fig. 13(e,f)].

Note that the relatively low flow rate q_{out} on 23 March 1998 (Table III) can be linked to the weather conditions: There was an intense snowfall on this day.

2. The pinch effect

In Sec. II B 1, it has been noted that there can be a lot of $F \rightarrow S$ transitions at $D6$, which do not lead to an occurrence of the congested pattern upstream of the on ramp [Fig. 4(d,e), arrows 1–3]. It has also been stressed that the pattern can occur only if the upstream front of the synchronized flow starts to propagate upstream (the up arrows *S* at $D5$ and $D4$ in Figs. 9–11).

However, in all investigated cases the general pattern upstream of the on ramp appears only if inside the synchronized flow upstream of the on ramp a compression of this synchronized flow occurs, i.e., if the pinch effect is realized. The time moment when this pinch effect at $D5$ has occurred is marked by the up arrow *P* in Fig. 9 ($D5$). In this case, the pinch effect occurs with a delay time (about 9 min) after the $F \rightarrow S$ transition has reached $D5$ (the up arrows *S* and *P* in Fig. 9, $D5$). On some other days, no such delay time has been observed: synchronized flow has already been compressed when the synchronized flow was measured at $D5$ (e.g., Fig. 11).

In the pinch region, the vehicle speed and the density change in a wide range [Fig. 9, $D5$ and Fig. 14(a)]. This spreading of the vehicle speed and of the density increase in the upstream direction inside the pinch region (Fig. 9, $D4$ and Fig. 14(c)]. This behavior has already been explained in

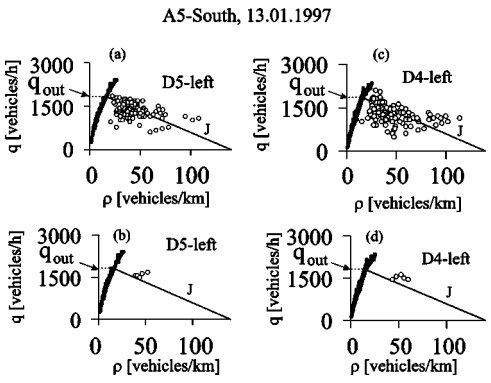

FIG. 14. The concatenation of measurement points for free flow (black points), the line *J*, and for synchronized flow in the pinch region (circles) in the flow-density plane for the highway A5-South [Fig. 3(a)] on 13 January 1997. (a, c) All points in the pinch region, (b, d) only some points between moving jams are shown.

TABLE III. Parameters of wide moving jams on three different days on the section of the highway A5-South

Parameter or characteristic	Day		
	15 April 1996	13 January 1997	23 March 1998
v_g (km/h)	−16	−15	−14
q_{out} (vehicles/h, left lane)	2000	1800	1650
q_{out} (vehicles/h, whole highway)	5000	4500	4200

Ref. [66] by the emergence of the growing narrow moving jams in the pinch region.

The fall of the average flow rate $q^{(pinch)}$ is observed after the pinch region is formed ($D5$, Fig. 15). It should be noted that this decrease in $q^{(pinch)}$ occurs earlier than the first wide moving jam is formed upstream of the pinch region ($D2, D1$). Therefore, the fall of the flow rate $q^{(pinch)}$ occurs inside the pinch region rather than this fall being caused by some possible decrease in the flow rate upstream of the pinch region. The interval of the averaging (10 min) in Fig. 15 ($D5$) is chosen to be higher than an average time distance between narrow moving jams that emerge in the pinch region (this distance between narrow moving jams is about 5–6 min at $D5$, see Sec. III C).

The fall of the average flow rate $q^{(pinch)}$ has a limit $q_{lim}^{(pinch)}$. After this limit has been achieved, the flow rate $q^{(pinch)}$ shows only small changes less than 10% in the vicinity of $q_{lim}^{(pinch)}$. This stationary feature of the pinch effect remains even if the flow rates to on ramps and the flow rate at $D6$ change during a long time interval shown in Fig. 15. However, the flow rate $q_{lim}^{(pinch)}$ can be noticeably different on different days (Table IV).

3. Correlation of flow rates in the outflow of wide moving jams and in the pinch region

To understand the latter empirical fact, the parameters of the pinch region and of the wide moving jams will be compared. First note [66] that inside the pinch region the traffic variables of synchronized flow that are measured during intervals between narrow moving jams are related to the points in the flow-density plane, which often lie above the line J [circles in Figs. 14(b) and (d)]. Nevertheless these points are related to the flow rates that are often lower than q_{out}. It turns out that $q_{lim}^{(pinch)}$ is correlated with q_{out}: the higher q_{out} is, the higher $q_{lim}^{(pinch)}$ is (Fig. 15). Besides, for all observed cases (Table IV)

$$q_{lim}^{(pinch)} < q_{out}. \tag{3}$$

The study on different days allows to suggest that

$$1.2 \lesssim q_{out}/q_{lim}^{(pinch)} \lesssim 1.5. \tag{4}$$

4. Pinch effect at the on ramp

It has been mentioned that the effective on ramp consists of two on ramps: $D6$-on and $D5$-on. The vehicle speed at the downstream on ramp $D6$-on remains almost without change after the $F \rightarrow S$ transition has occurred at $D6$ ($D6$-on in Figs. 9–11). However, at the upstream on ramp $D5$-on the pinch effect that is very similar to the one on the highway ($D5$) on 13 January 1997 and on 23 March 1998 is realized when the flow rate to this on ramp increases ($D5$-on in Figs. 9 and 11). This pinch effect occurs often with a delay time after the $F \rightarrow S$ transition reaches $D5$. It has been found that apparently due to this pinch effect at the on ramp $D5$-on, as well as on the highway ($D5$) the flow rate to the on ramp $D5$-on

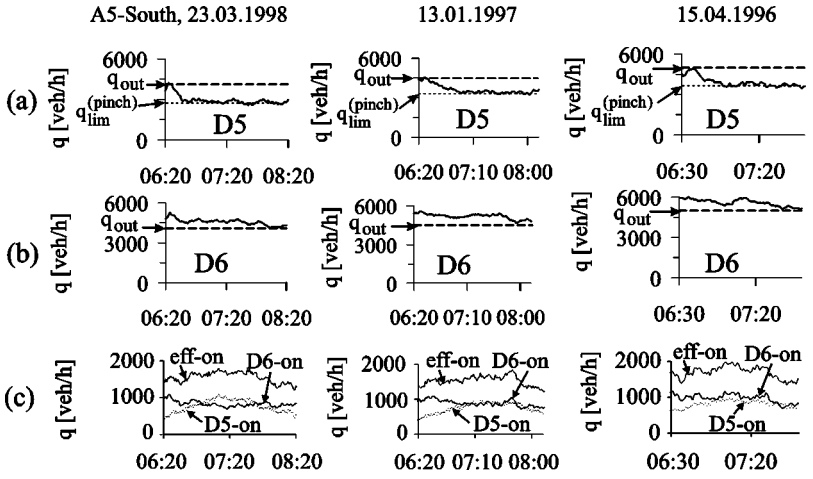

FIG. 15. The average flow rate inside the pinch region $q^{(pinch)}$ (solid curves) (a), the discharge flow rate $q_{out}^{(bottle)}$ (b), and the flow rates to the on ramps $D5$-on, $D6$-on, and $q_{eff\text{-}on}$ (''eff-on'') (c) for three different days. 10 min averaged data: each 10 min averaged value is set to the minute at which the 10 min interval of the averaging begins. Dashed lines in (a, b) are related to the flow rate in the outflow of a wide moving jam when free flow is formed downstream of the jam, q_{out}.

TABLE IV. The limit flow rate in the pinch region of the general pattern on three different days on the section of the highway A5-South.

Parameter or characteristic	Day		
	15 April 1996	13 January 1997	23 March 1998
$q_{lim}^{(pinch)}$ (vehicles/h whole highway)	3700	3400	2800
$q_{out}/q_{lim}^{(pinch)}$	1.35	1.32	1.5

changes less than 12% in the vicinity of a limit value after the pinch effect has occurred there [$D5$-on, Fig. 15(c)].

5. Influence of wide moving jam emerging in the pinch region on the general pattern

As it has been noted, wide moving jams are usually formed at the distance $L_{syn} \approx 3-4$ km upstream of $D6$. Now a somewhat exceptional case is considered, when a wide moving jam appears upstream but very close to the effective bottleneck at $D6$. The wide moving jam is marked by the down arrow "B" in Fig. 16(a).

The wide moving jam "B" occurs between $D6$ and $D5$. Indeed, at $D6$ and at $D6$-on the vehicle speed does not fall either before or after the jam is measured at $D5$ and $D5$-on [Fig. 16(a)]. After the jam has occurred, it propagates through the general pattern ($D5$–$D1$, down-arrow "B"). The occurrence and propagation of the jam causes two effects.

The first effect is the return $S \rightarrow F$ transition at the effective bottleneck [$D6$, up arrow F_1 in Fig. 16(a) and the arrow at 08:35 in Fig. 16(c)]. The jam occurs upstream of $D6$ but very close to $D6$. Therefore, the flow rate at $D6$ during the jam formation decreases [Fig. 16(b), $D6$]. This may explain the return $S \rightarrow F$ transition. When the jam propagates upstream of $D5$, the flow rate at $D6$ increases (it is the sum of the flow rate out from the jam B and $q_{eff\text{-}on}$) and a new $F \rightarrow S$ transition at $D6$ occurs [$D6$, up arrow S_2 in Fig. 16(a,b) and the arrow at 08:43 in Fig. 16(d)].

The second effect is the suppression of the growth of narrow moving jams in the pinch region, which are very close to the downstream front of the jam B. Apparently due to this effect the moving jams "1" and "2" disappear [$D5$–$D3$ in Fig. 16(a)]. This suppression effect is apparently the same as the one in the vicinity of the upstream front of the synchronized flow in GP [66].

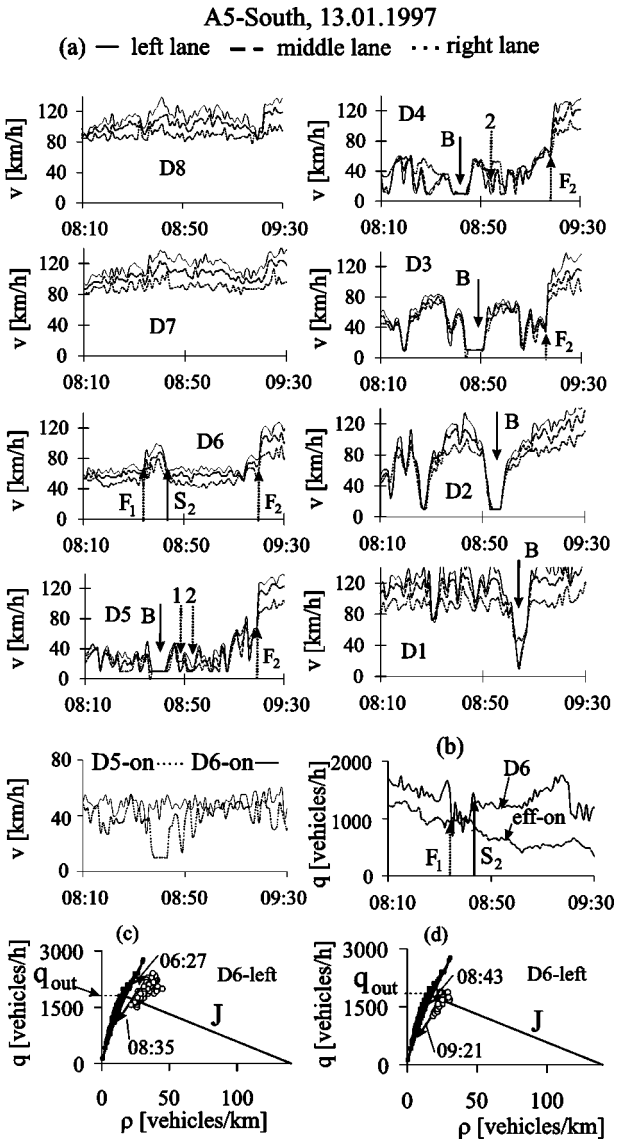

FIG. 16. Hysteresis phenomena at the on ramp. The vehicle speed (a) and the flow rate (b) on different detectors on the highway A5-South [Fig. 3(a)] on 13 January 1997. (c, d) Hysteresis phenomena in the flow-density plane due to the $F \rightarrow S$ transitions and the reverse $S \rightarrow F$ transitions at the on ramp ($D6$). Free flow (black points) and synchronized flow (circles).

C. Emergence of moving jams

1. Stationary and temporal features of the pinch effect

The pinch effect shows both some stationary and some temporal features. The stationary feature of the average flow rate $q^{(pinch)}$ has already been stressed in Sec. III B 2 [Fig. 15(a)]. However, if 1 min data are considered, the emergence of growing narrow moving jams in the pinch region, which propagate upstream can be found out. The features of this temporal effect have already been considered in Ref. [66].

In particular, it has been mentioned that if the mean distance between the narrow moving jams in the pinch region $\overline{R}_{narrow}$ is lower than some minimum distance between wide moving jams (about 2.5 km) then some of these narrow jams disappear during their transformation into wide moving jams. As a result, the mean distance between wide moving jams ($D1$) is noticeably higher than the initial distance between narrow jams ($D5$). This result [66] is also valid for all three days under consideration (see Figs. 9–11 and Table V).

Nevertheless, even the temporal process of the narrow moving jams dynamics in the pinch region possesses a stationary feature. The mean time distance between narrow

TABLE V. The mean time distance between moving jams T_J and period of speed correlation functions T_c at different locations

Day	Detectors	$D1$	$D2$	$D3$	$D4$	$D5$
15 April 1996	T_J (min)	11.2	9.3	8.2	6.2	5
	T_c (min)	10.5	11	11	9.2	4.9
13 January 1997	T_J (min)	15.7	8.1	7.1	5.2	6.3
	T_c (min)	9.7	6.4	6.6	6.2	7.1
17 March 1997	T_J (min)	17	17	10	6.3	5.5
	T_c (min)	22	16.7	7.5	7.3	6.1
23 March 1998	T_J (min)	9.9	8.1	7	5.5	5.2
	T_c (min)	8.3	7.8	7.4	5.7	4.8
20 April 1998	T_J (min)	12.8	11.2	10.6	7.1	5.3
	T_c (min)	17.7	19.2	14.8	5.9	5.4

moving jams T_J when they are just emerging (at $D5$) is related to the limit (minimum) mean time distance $T_{J,\,lim}$, which is about 5–7 min for different days (Table V, $D5$). This value of $T_{J,\,lim}$ is correlated with the minimum of the mean distance between narrow jams $\overline{R}_{narrow}$ in Fig. 2(b) in Ref. [66]. This mean minimum distance is about 1.5 km. This corresponds to the time distance between narrow jams $T_{J,\,lim}=6$ min at $D5$ at the narrow jam velocity -15 km/h.

The other stationary feature of the pinch effect is the following. The mean time from the narrow moving jam emergence till the $S\rightarrow J$ transition, i.e., till the transformation of a narrow moving jam into a wide moving jam, T_{narrow}, is also a nearly constant value for different moving jams on the same day (exactly for the same traffic conditions), e.g., it is about $T_{narrow}\approx 11$ min on 13 July 1997.

However, these stationary features are valid only during the time interval when the average flow rate $q^{(pinch)}$ is also nearly constant in the vicinity of $q_{lim}^{(pinch)}$ [Fig. 15(a)].

It must also be noted that the time T_{narrow} needed for the $S\rightarrow J$ transition (about 10–12 min) is considerably longer than the time needed for the $F\rightarrow S$ transition (about 1 min, see Sec. II B). The high value T_{narrow} and complex dynamics of the wide moving jam emergence may be responsible for the strong spatial dependence of the speed correlation function, which will be considered below.

2. Spatial dependence of speed correlation function

The speed correlation function for moving jams (''stop-and-go-traffic'') has already been studied in Ref. [61]. In Ref. [61], it has been found that the period of this function is about 10 min.

It is interesting to analyze the speed correlation function during the moving jam emergence at different locations (Fig. 17 and Table V). It can be seen from Table V that the speed correlation function, which is calculated during the wide moving jam emergence for the different locations ($D5$–$D1$), strongly depends on the spatial coordinate. The period of this function can change in space from about 5 min up to about 20 min.

The speed correlation function is calculated for time series $v_n=v(t_n)$ where v is the vehicle speed, $t_n=n\Delta t+t_0$ is

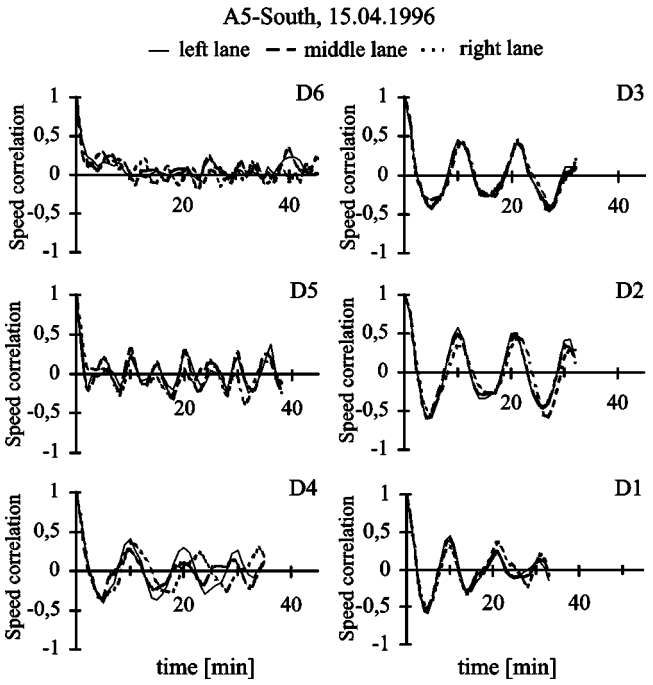

FIG. 17. Spatial dependence of the speed correlation function (5) during the moving jam emergence upstream of the effective bottleneck at $D6$ on 15 April 1996 on the section of the highway A5-South [Fig. 3(a)]: the speed correlation function at different detectors.

the time within a given time interval $t_0<t_n\leqslant t_N$, $n=1,2,\ldots,N$, $\Delta t=1$ min, t_0 is an initial time, and N is the number of points in the interval. The correlation function $R_{VV}(k\Delta t)$, $k=0,1,2\ldots$, is determined as [79]

$$R_{VV}(k\Delta t)=\frac{1}{\sigma^2(N-k)}\sum_{n=1}^{N-k}(v_n-\langle v\rangle)(v_{n+k}-\langle v\rangle), \quad (5)$$

where $\langle v\rangle$ is the average speed over time interval $t_0<t_n\leqslant t_N$,

$$\langle v\rangle=\frac{1}{N}\sum_{n=1}^{N}v_n, \quad \sigma^2=\frac{1}{N}\sum_{n=1}^{N}(v_n-\langle v\rangle)^2. \quad (6)$$

The maximal value of the number k in formula (5) for $R_{VV}(k\Delta t)$ is chosen equal to N/2.

The period of this function T_c (Table V) has a minimum from about 5 up to 7 min for different days in the pinch region ($D5$). This period increases with the increase in the amplitude of the moving jams reaching the maximum value (from about 9 min up to about 20 min for the different days) when the narrow jams have been transformed into the wide moving ones. Besides, while the period of the speed correlation function T_c is nearly the same in the pinch region of the general pattern ($D5$) on all days, this period is very different for wide moving jams that have formed on these different days ($D1$). Note that from the results in Table V it can be concluded that in some case, e.g., on 20 April 1998, the mean time distance between moving jams T_J is lower than

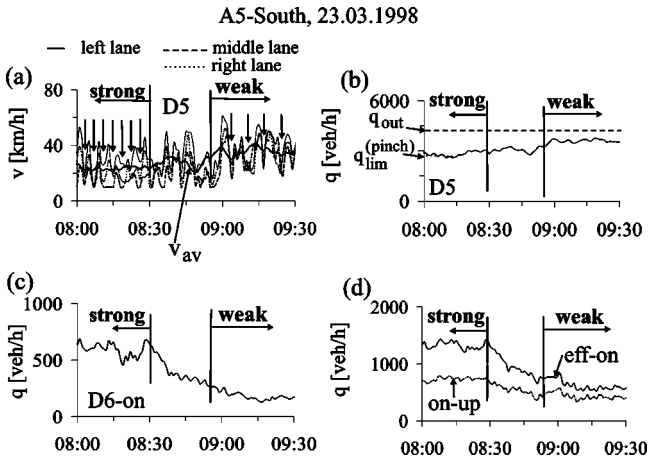

FIG. 18. Transition from the strong congestion to the weak one. (a) The vehicle speed for different lanes (1 min data) where narrow moving jams are marked by down arrows and the average speed v_{av} (thick solid curve, 10 min averaged data). The flow rates in the pinch region ($D5$) (b), to the on ramp $D6$-on (c), to the effective on ramp (eff-on), and the upstream part of the flow rate to the effective on ramp $q_{on\text{-}up}=q_{eff\text{-}on}-q_{D6\text{-}on}$ (on-up) (d) (10 min data: each 10 min averaged value is set to the minute at which the 10 min interval of the averaging begins). Data from 23 March 1998, A5-South.

the period of the correlation function T_c. This is because the moving jams of lower amplitude decrease the average time distance between the moving jams T_J, but they only slightly influence the period of the speed correlation function.

IV. EVOLUTION OF GENERAL PATTERNS AT ON RAMPS

A. "Strong" and "weak" congestion: The definition

The time dependence of the flow rate $q_{eff\text{-}on}(t)$ has the maximum point $q_{eff\text{-}on,\,max}$ at the time $t=t_{eff\text{-}on}$. This time is later than the time $t=t_{FS}$ of the general pattern emergence (Table II and Fig. 12, eff-on). Whereas $q_{eff\text{-}on}$ is changing at a high level in the vicinity of $q_{eff\text{-}on,\,max}$, the average flow rate in the pinch region $q^{(pinch)}$ is self-maintained near the limit (minimal) flow rate $q_{lim}^{(pinch)}$ and the average vehicle speed v_{av} is low [the region "strong" in Figs. 18(a,b)]. This case will be called the "strong" congestion. In the strong congestion, the initial mean time distance between narrow moving jams reaches the lowest possible value $T_{J,\,lim}$ and the mean width of the synchronized flow in GP L_{syn} is limited, and this width is independent of traffic demand. Thus, the pinch effect considered in Sec. III is related to the strong congestion condition.

In contrast, when the flow rate $q_{eff\text{-}on}$ decreases below some value, the average speed in the pinch region v_{av} begins to increase gradually and the flow rate $q^{(pinch)}$ loses the property to be a self-maintaining value close to $q_{lim}^{(pinch)}$ (Fig. 18). This case will be called the "weak" congestion. Under the weak congestion, the time distance between emerging narrow moving jams increases with the increase in the average speed in the pinch region [Fig. 18(a)]. This is correlated with Ref. [66], where it has been found that the higher the speed in the pinch region away from narrow moving jams is, the higher is the mean initial distance between narrow jams $\overline{R}_{narrow}$.

The distance $\overline{R}_{narrow}$ can be sometimes equal to or higher than the minimum time distance between wide moving jams. Thus, each growing narrow moving jam can lead to the occurrence of a wide moving jam. If the speed in synchronized flow is high enough then no moving jams emerge in this flow.

It will be shown below that under the weak congestion diverse transformations between different congested patterns can occur.

B. Synchronized flow pattern

When the flow rate $q_{eff\text{-}on}$ decreases below some value, GP can gradually transform into SP (Fig. 19). On 23 March 1998 this transformation occurs in the time interval from 9:00 up to 9:20, when the flow rate $q_{eff\text{-}on}$ is related to the flow rate interval designated $q_{eff\text{-}on}^{(trans)}$ in Table II. Upstream of SP, free flow occurs [$D1$, Fig. 19(b), middle], i.e., this SP is localized at the bottleneck. Such a pattern is called the LSP. Wide moving jams do not emerge in SP. In comparison with GP, in SP the average speed and the flow rate are considerably higher at $D5$ [Fig. 19(c)]. Thus, in SP the weak congestion is realized.

C. Alternations of free and synchronized flows in congested patterns

During the time interval from 9:20 up to 9:41, when the localized SP occurs [Fig. 19(b), middle], the flow rate $q_{eff\text{-}on}=570$–615 vehicles/h. When $q_{eff\text{-}on}$ is further decreased [$q_{eff\text{-}on}$ is 390–420 vehicles/h during 9:42–9:50], local regions of free flow ($D5, D4$) appear, which spatially alternate with local regions of synchronized flow ($D3$) [Fig. 19(b), right]. However, synchronized flow is self-maintained at the bottleneck ($D6$). Besides, wide moving jams emerge in the most upstream region of synchronized flow inside the pattern [$D2$ and $D1$ in Fig. 19(b), right]. Thus, this pattern may be considered as a variant of (GP). Inside this GP, local regions of free flow spatially *alternate* with local regions of synchronized flow [marked "AGP" in Fig. 19(b), right].

Note that the flow rate $q_{eff\text{-}on}$ increased up to 600 vehicles/h during 9:57–9:59. At such a flow rate $q_{eff\text{-}on}$ SP could exist [Fig. 19(c)]. However, SP does not occur anymore.

The appearance of free flow at $D5$ and $D4$ may be explained by the occurrence of the return $S\rightarrow F$ transition inside the initial SP when the flow rate $q_{eff\text{-}on}$ is decreasing [Fig. 19(c)]. However, because synchronized flow at the bottleneck ($D6$) is still self-maintained, the discharge flow rate ($D6$) remains at approximately the same level as in SP [Fig. 19(c)]. Thus, it may be assumed that the downstream front of GP [this GP is marked as "AGP" in Fig. 19(b), right] is located at the bottleneck ($D6$) as well as the downstream front of the initial GP and SP.

There may be also the following interpretation of the phenomenon of the appearence of alternations of free and syn-

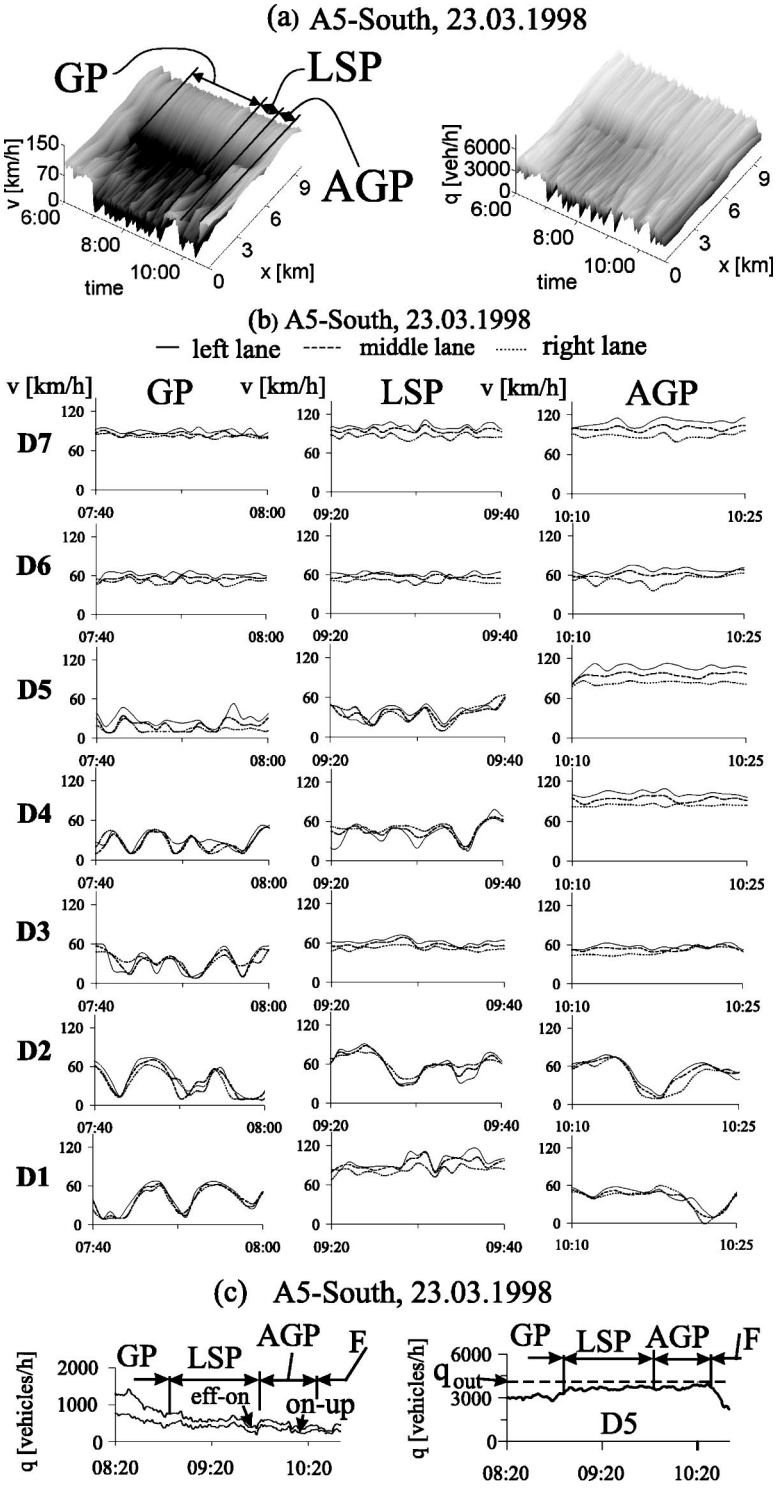

FIG. 19. Evolution of the general pattern (GP) into the localized synchronized flow pattern (LSP) and then into GP where a spatial alternation of free and synchronized flows occurs (marked ''AGP'') due to a decrease in the flow rate to the effective on ramp upstream of the bottleneck at $D6$ on 23 March 1998 on the section of the highway A5-South [Fig. 3(a)]. (a) Overview. (b) The vehicle speed on different detectors: GP (left), LSP (middle) and AGP (right). (c) The flow rates at different detectors (10 min averaged data): ''eff-on'' and ''on-up'' are the flow rates to the effective on ramp $q_{eff\text{-}on}$ and the flow rate $q_{on\text{-}up}=q_{eff\text{-}on}-q_{D6\text{-}on}$, respectively. F free flow.

chronized flows in congested patterns. It can be seen in Fig. 19(a) that synchronized flow in AGP appears due to a spatial separation of synchronized flow in the initial LSP. Exactly, AGP may be considered as two different patterns: (i) LSP, localized in the vicinity of the bottleneck [$D6$, Fig. 19(b), right] and (ii) a MSP. When synchronized flow in this MSP is far enough from the bottleneck ($D3$–$D1$), wide moving jams emerge in this synchronized flow.

On other days, the evolution of GP when the flow rate $q_{eff\text{-}on}$ decreases can show qualitatively similar pictures as on 23 March 1998 (Fig. 19). However, sometimes rather than GP the SP, where local regions of free flow spatially alternate with local regions of synchronized flow, occurs. The latter SP may also be interpreted as two different patterns: (i) LSP at the bottleneck and (ii) MSP where no wide moving jams occur.

Sometimes, an initial GP transforms into LSP that dissolves later. In some other cases, an appearance of free flow inside the synchronized flow of the initial GP (or SP) leads to the occurrence of MSP.

D. Hysteresis phenomena at the effective bottleneck during the pattern formation and dissolution

While the $F \rightarrow S$ transition at the effective bottleneck is accompanied by the fall in the vehicle speed [e.g., Fig. 4(a–c)], the return $S \rightarrow F$ transition is accompanied by the jump of the speed. Therefore, both first order phase transitions cause the well-known hysteresis effect [Figs. 16(c,d)]. On 13 January 1997, due to the appearance of a wide moving jam between $D6$ and $D5$, which causes the return $S \rightarrow F$ transition at $D6$ without the dissolution of the general pattern, there are two hysteresis effects (Sec. III B 5).

However, usually the $S \rightarrow F$ transition occurs due to the dissolution of the congested pattern. One of the scenarios of this dissolution is shown in Fig. 16(a). A wave of the return $S \rightarrow F$ transitions starts upstream of the congested pattern and propagates downstream (up arrows F_2, $D3$–$D5$) up to the effective bottleneck [$D6$, up arrow F_2 and the arrow at 9:21 in Figs. 16(a) and 16(d), respectively]. As a result, the congested pattern dissolves and free flow occurs at the bottleneck [Fig. 16(a)].

When GP or SP occur where local regions of free flow spatially alternate with local regions of synchronized flow, a different scenario of the congested pattern dissolution is possible. On 23 March 1998 the dissolution of synchronized flows at $D6$ and at $D3$–$D1$ in AGP begins almost simultaneously (up arrows F_1 and F_2 at 10:31, $D6$ and $D1$ in Fig. 11). However, because synchronized flow at $D3$–$D1$ is extended over about 3 km, this synchronized flow dissolves later due to the wave of the $S \rightarrow F$ transitions, which propagates downstream from the detectors $D1$ to $D2$ and then to $D3$ (up arrows F_2 at $D2$ and $D3$). As a result, the dissolution finishes at $D3$ three minutes later (at 10:34) than it has begun at $D1$. There may be another explanation of this pattern dissolution. This explanation is based on the above assumption that the AGP in Fig. 19 consists of two patterns: LSP at the bottleneck and MSP. Thus, these two patterns dissolve independently of each other due to two different waves of the return $S \rightarrow F$ transitions.

E. Discharge flow rate and highway capacity

There are three kinds of highway capacity depending on which phase traffic is in. These kinds of highway capacity are the following [66]. (1) The capacity of free flow is $q_{max}^{(free)}$. (2) The capacity downstream of synchronized flow at a bottleneck is related to the maximal possible discharge flow rate $q_{out,max}^{(bottle)}$. (3) The capacity downstream of a wide moving jam is q_{out} (Table III). These capacities have a probabilistic nature, because of local first order phase transitions between three traffic phases.

Recall that [70]

$$q_{max}^{(free)}/q_{out} \approx 1.5. \tag{7}$$

Thus, for the general patterns at on ramps, one derives from Eqs. (4) and (7) the following empirical relation:

TABLE VI. The maximal $q_{out,max}^{(bottle)}$ and the minimal $q_{out,min}^{(bottle)}$ discharge flow rates on three different days on the section of the highway A5-South. Both flow rates are measured during the time interval when the congested pattern exists at the effective bottleneck at $D6$. 1 min averaged data across the whole highway.

Parameter or characteristic	Day		
	15 April 1996	13 January 1997	23 March 1998
$q_{out,max}^{(bottle)}$ (vehicles/h)	6840	6180	5220
$q_{out,min}^{(bottle)}$ (vehicles/h)	4500	3540	3420
$q_{out,max}^{(bottle)}/q_{out}$	1.37	1.37	1.24
$q_{out,min}^{(bottle)}/q_{out}$	0.9	0.79	0.81

$$1.8 \lesssim q_{max}^{(free)}/q_{lim}^{(pinch)} \lesssim 2.25. \tag{8}$$

The maximal and minimal values of the discharge flow rate $q_{out}^{(bottle)}$ during the time when the congested pattern existed at the bottleneck have been measured both for 1 min (Table VI) and for 10 min averaged data (to show mean results) (Table VII). It can be seen that $q_{out}^{(bottle)}$ can change in a wide range $[q_{out,\,max}^{(bottle)}, q_{out,\,min}^{(bottle)}]$. Besides, the maximum value $q_{out,\,max}^{(bottle)}$ can noticeably exceed the flow rate out of a wide moving jam q_{out}, whereas $q_{out,\,min}^{(bottle)}$ can be lower than q_{out}.

Because in GP under the strong congestion the flow rate $q^{(pinch)}$ has only small changes near $q_{lim}^{(pinch)}$, the average discharge flow rate (2) should change correspondingly to the change in the flow rate to the effective on ramp $q_{eff\text{-}on}$. This behavior is indeed observed in the empirical study [Fig. 15(b)].

V. CONGESTED PATTERNS AT OFF RAMPS

All types of patterns that occur at an isolated on ramp can also occur at an isolated off ramp. However, congested pat-

TABLE VII. The same parameters and characteristics as in Table VI but for 10 min averaged data across the whole highway.

Parameter or characteristic	Day		
	15 April 1996	13 January 1997	23 March 1998
$q_{out,max}^{(bottle)}$ (vehicles/h)	5940	5420	4880
$q_{out,min}^{(bottle)}$ (vehicles/h)	5140	3640	3920
$q_{out,max}^{(bottle)}/q_{out}$	1.19	1.2	1.16
$q_{out,min}^{(bottle)}/q_{out}$	1.03	0.8	0.93

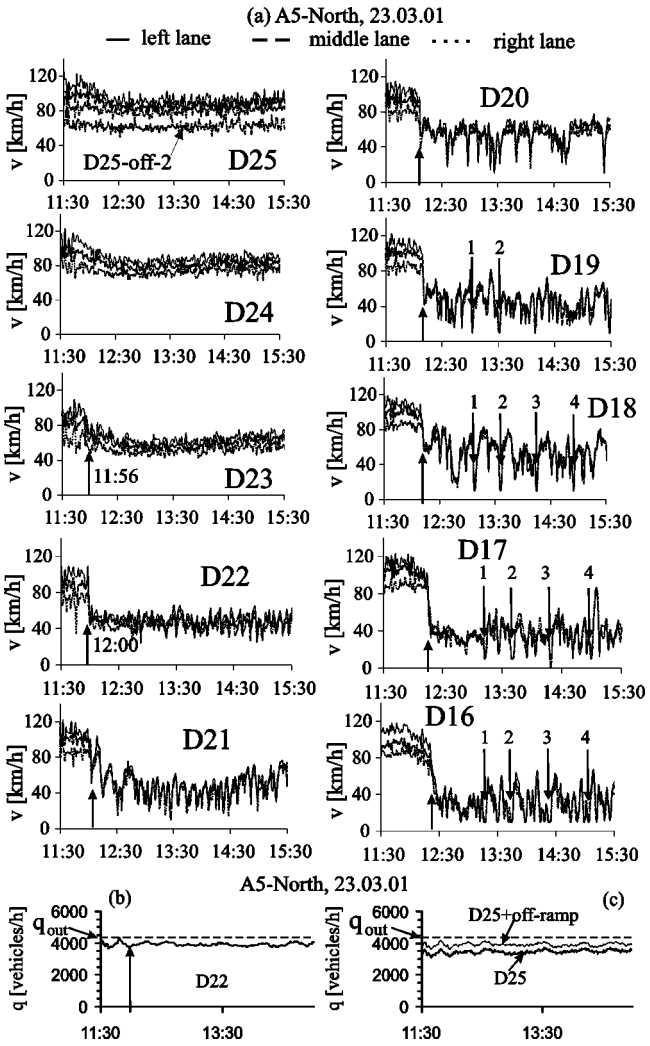

FIG. 20. The general pattern (GP) at the isolated bottleneck at the off ramp $D25$-off on 23 January 2001 on the section of the highway A5-North [Fig. 3(c)]. (a) The vehicle speed on different detectors (1 min data). The flow rate in the pinch region (b) and the discharge flow rate (''$D25+$ off ramp'') (c) for GP (10 min intervals data). The up arrow in (b) symbolically shows the time of the $F \rightarrow S$ transition, which leads to GP formation.

terns at the off ramp [Fig. 20(a)] and their evolution (Fig. 21) show some peculiarities.

A. The general pattern

First, upstream of the off ramp $D25$-off on A5-North the $F \rightarrow S$ transition at $D23$ [up arrow in Fig. 20(a)] occurs (the reason of the $F \rightarrow S$ transition is the same as it has been discussed in Sec. II C). The following upstream propagation of the synchronized flow (up arrows at $D22$, $D21$) leads to the formation of GP where the synchronized flow pattern occurs and wide moving jams emerge in that synchronized flow [down arrows in Fig. 20(a), $D19$–$D16$].

However, in the pinch region of this GP the weak congestion condition is realized. Indeed, in contrast to GP at $D6$ considered in Sec. III (Figs. 9–11), in GP at the off ramp $D25$-off on A5-North there is almost no difference between the flow rate at $D22$ in free flow regime [the time interval before the up arrow in Fig. 20(b)] and in the pinch region at $D22$ (the time interval after the up arrow). In the pinch region, the vehicle speed away from moving jams [about 40–60 km/h, Fig. 20(a), $D22$, $D21$] is noticeable higher than in the pinch region of GP at the on ramp under the strong congestion (about 20–30 km/h, Figs. 9–11, $D5$).

The upstream front of synchronized flow in GP at the off ramp is continuously widening upstream [up arrows in Fig. 20(a)]. Therefore, the width L_{syn} of the synchronized flow in GP at the off ramp is increasing over time rather than it being spatially limited. In contrast to GP at the on ramp considered in Sec. III A 2 (Figs. 9–11), the upstream boundary of synchronized flow in the GP at the off ramp in Fig. 20 is not determined by the location of the $F \rightarrow S$ transition (the wide moving jam emergence). First, synchronized flow propagates continuously upstream of the bottleneck (up arrows in Fig. 20) and only later wide moving jams emerge in this synchronized flow.

B. Transformations between different types of congested patterns

It has been found that the weak congestion is the usual case for different congested patterns at off ramps. In particular, the weak congestion occurs in the MSP shown in Fig. 6(a) and in all other congested patterns shown in Figs. 21 and 22. Under the weak congestion diverse transformations between different types of congested patterns often occur over time.

For example, GP at off ramps can easily transform into one of the synchronized flow patterns. Either the LSP, or the widening SP (WSP), i.e., SP whose upstream front is continuously widening upstream, or else MSP can occur. Besides, in both GP and SP (LSP or WSP) local regions of free flow, which spatially alternate with regions of synchronized flow are often realized. An example is shown in Fig. 21 where GP first transforms into GP with such an alternation of free and synchronized flows (marked ''AGP'') and then later once again GP without this alternation occurs. However, in this AGP almost free flow conditions are at $D23$–$D21$, i.e., this AGP may also be interpreted as GP whose downstream boundary has moved upstream from the initial effective location of the bottleneck in the vicinity of $D23$ to $D20$.

At some off ramps, GP exist only during short time intervals. There are relatively frequent transformations between different congested patterns. Such a case is usually realized upstream of the off ramp $D23$-off on the highway A5-South (Fig. 22). It can be seen that GP, where only one wide moving jam is formed, transforms into SP, then GP once again appears.

VI. COMPLEX PATTERN FORMATION CAUSED BY PECULIARITIES OF HIGHWAY INFRUSTRUCTURE

A. "Foreign" wide moving jams

A real highway has a lot of effective bottlenecks. Thus, two or more general patterns where the related different se-

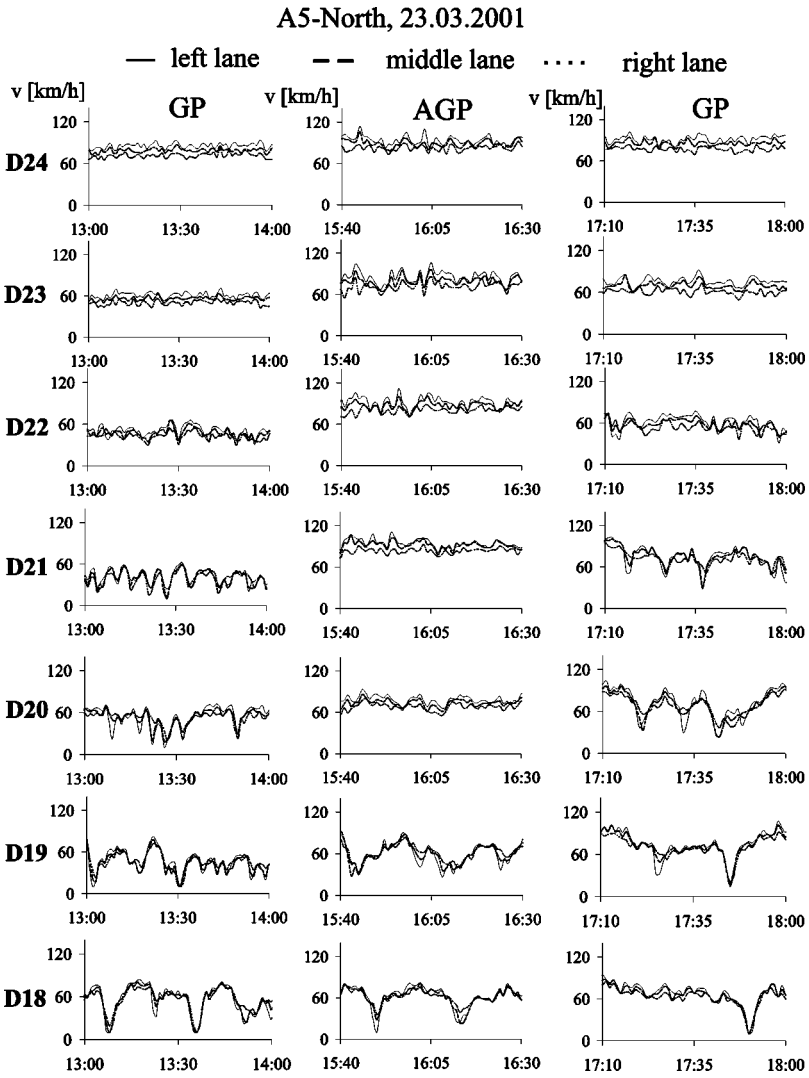

FIG. 21. Evolution of congested patterns that occur at the isolated bottleneck at the off ramp *D*25-off on 23 January 2001 on the section of the highway A5-North [Fig. 3(c)]. The vehicle speed on different detectors. GP is the general pattern (left and right) and AGP is the GP where a spatial alternation of free and synchronized flows occurs (middle).

quences of wide moving jams emerge can appear almost simultaneously. The wide moving jams from downstream sequences of wide moving jams will be called *"foreign" wide moving jams* [the jams marked by the down arrows ''*A*'' and ''*B*'' in Fig. 3(b) and Fig. 23] when they propagate through an upstream general pattern (GP at *D*6) where other narrow moving jams are just emerging (the jams marked by the down arrows 1–9 in Fig. 23).

Upstream of the ''foreign'' wide moving jam *A*, the narrow jam emergence is not influenced by this ''foreign'' jam. Downstream of the foreign wide moving jam *A*, the narrow jams marked by the arrows 6 and 7 disappear. This suppression effect is apparently the same as the suppression of narrow jams by a wide jam at the upstream boundary of the pinch region (see Sec. III A 2) [66]. However, far enough downstream from the jam *A* the features of the jam emergence are not influenced by the foreign wide moving jam propagation. Thus, the narrow jam marked by the arrow 8, which is far enough downstream of the foreign jam *A* grows leading to the formation of the wide moving jam 8 at *D*2 (Fig. 23). All mentioned features of the foreign wide moving jam *A* propagation are characteristic for all other foreign wide jams, in particular for the wide moving jam *B*.

As a result of these effects, instead of initial isolated sequences of wide moving jams (the foreign wide moving jams *A* and *B* and the jams marked by the arrows 1–8) a united sequence of wide moving jams is finally formed (down arrows 1 3 *A* 8 *B* in Fig. 23, *D*2, *D*1).

B. "Expanded" congested patterns

1. The definition and some common features

If two or more effective bottlenecks exist close to one another on a highway, then a congested pattern can occur where synchronized flow covers several effective bottlenecks. This pattern will be called *the expanded congested pattern* (EP).

The empirical study shows that in some cases two or more spatially separated pinch regions can occur in the synchronized flow of EP. Each of these pinch regions occurs upstream of the related effective bottleneck.

In a lot of other cases, EP are observed where the pinch region covers two or more effective bottlenecks. The width of this expanded pinch region can be much higher than the width of the pinch region occurring upstream of an isolated bottleneck. In these cases, narrow wide moving jams after

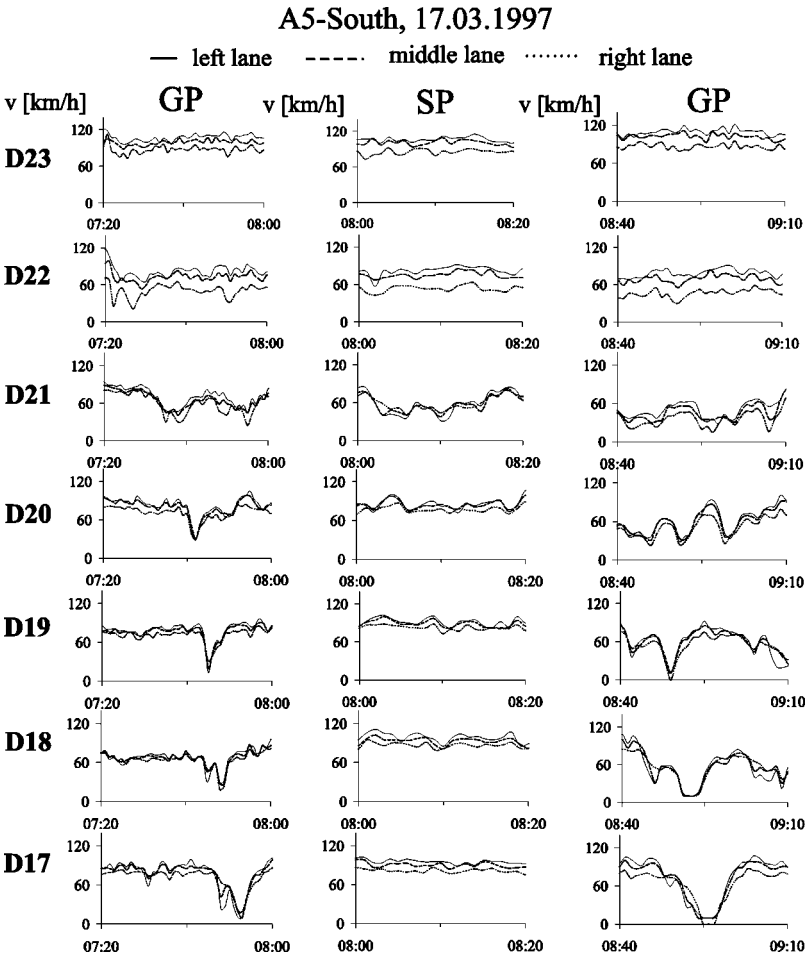

FIG. 22. Evolution of congested patterns that occur upstream of the off ramp $D23$-off on 17 March 1997 on the section of the highway A5-South [Fig. 3(a)]. The vehicle speed on different detectors. GP is the general pattern and SP is the synchronized flow pattern.

they have emerged can remain the narrow jams during the propagation through the whole expanded pinch region without transformation into the wide moving jams. Naturally, intermediate cases where some of the pinch regions are separated and the others cover several effective bottlenecks are observed.

EP can also have a spatial-temporal structure qualitatively similar to (GP) at an isolated bottleneck. However, the empirical study shows that there are some important peculiarities of EP. First, because synchronized flow in EP covers several bottlenecks, the pinch region can be much longer than in the case of an isolated bottleneck. Second, a lot of ''foreign'' wide moving jams that are formed inside different pinch regions between different bottlenecks can propagate through EP.

2. An example of EP

In Sec. V A it has already been mentioned that upstream of the effective bottleneck $B_{North\,1}$ [Figs. 3(c,d)] GP is formed [Fig. 20(a)]. The upstream front of the synchronized flow in this GP propagates upstream [up arrows, $D23$–$D17$]. After this front reaches the effective bottleneck $B_{North\,2}$ at the on ramp ($D16$), the $F \rightarrow S$ transition at the latter bottleneck occurs [up arrow in Fig. 20(a), $D16$]. As a result, the synchronized flow propagates further upstream [up-arrows in Fig. 24, $D15$, $D14$] covering both bottlenecks. Therefore, EP occurs whose overview is shown in Fig. 3(d).

In this expanded pattern, there are two spatially separated pinch regions in the synchronized flow. The first pinch region has been formed between the bottleneck $B_{North\ 1}$ and the bottleneck $B_{North\,2}$ [Fig. 20(a)]. In this pinch region, wide moving jams occur downstream of the bottleneck $B_{North\,2}$ [Fig. 20(a), $D17$, up arrows]. These wide moving jams [the down arrows 1–4 in Fig. 20(a) and Fig. 24] that propagate further upstream can be considered as foreign wide moving jams for the second pinch region upstream of the bottleneck $B_{North\,2}$ where other narrow moving jams emerge.

In the case shown in Fig. 24, the strong congestion occurs in the pinch region ($D15$) upstream of the bottleneck $B_{North\,2}$ ($D16$). As a result, the upstream propagation of the upstream front of synchronized flow is spatially limited and the front is located between $D11$ and $D12$. A region of wide moving jams is formed between $D11$ and $D12$, i.e., at approximately the same distance (about 4 km) from the effective bottleneck at $D16$ as in the case of the effective bottleneck at $D6$ on the highway A5-South (e.g., Fig. 9).

However, these wide moving jams are not the reason for the $F \rightarrow S$ transition at the next upstream bottleneck $B_{North\,3}$ ($D7$). This transition is earlier induced by the upstream propagation of the local region of synchronized flow, which has originally appeared at $D12$ (up arrow at 11:59). Therefore, the wide moving jams are also the foreign jams for the congested pattern that is formed upstream of this third effective bottleneck ($D6$ in Fig. 24).

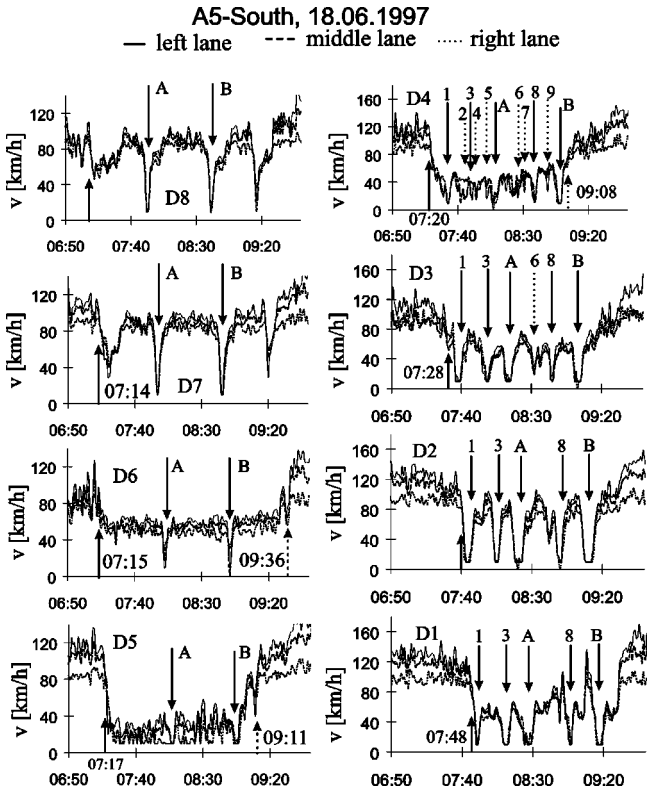

FIG. 23. Explanation of ''foreign'' wide moving jams. The propagation of the ''foreign'' wide moving jams ''*A*'' and ''*B*'' through the general pattern. The vehicle speed at different detectors. GP has been formed due to the $F \rightarrow S$ transition at 07:15 at the on ramp (up arrow, $D6$) induced by the propagation of a local region of synchronized flow (up arrow, $D7$) on 18 June 1997 on the section of the highway A5-South [Fig. 3(a)]. The overview of this ''foreign'' wide moving jam propagation through GP at the bottleneck B_3 is shown in Fig. 3(b).

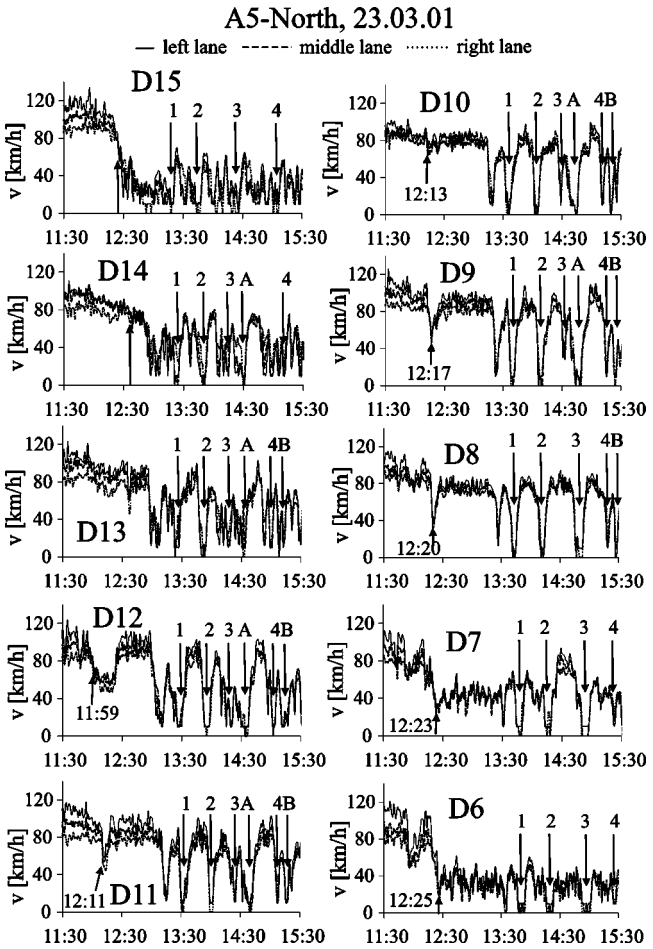

FIG. 24. A part of the expanded pattern (EP) upstream of the bottleneck $B_{North\,2}$ at $D16$ (the on ramp) on 23 January 2001 on the section of the highway A5-North [Fig. 3(c)]: The vehicle speed at different detectors. The downstream part of this EP (downstream of the bottleneck at $D16$) is shown in Fig. 20. The overview of the EP can be seen in Fig. 3(d).

C. Dissolution of moving jams at bottlenecks

There are bottlenecks that do not appear to be effective ones, i.e., the $F \rightarrow S$ transition is not observed there. If a foreign moving jam that has initially occurred downstream of the bottleneck propagates through this bottleneck either the width of the jam can decrease or the jam can dissolve. Indeed, let us assume that the bottleneck is linked to a decrease in the number of highway lanes from ''m'' to ''n'' in the direction of traffic flow ($n<m$). Then the flow rate in the outflow from the foreign wide moving jam q_{out} increases when the jam propagates through the bottleneck correspondingly to the ratio m/n but the flow rate into the jam q_{in} can remain the same. The dissolution of the foreign wide moving jams at such a bottleneck (where $m=3$ and $n=2$) is observed on the German highway A1 [Figs. 25(a,b)]. First, the moving jams (marked by down arrows 1–3) are on the two-lane section of the highway ($D8$). After the jams due to their upstream propagation reach the three-lane section of the highway they begin to dissolve gradually ($D7, D5$). Finally, the jams have dissolved and free flow occurs at $D3$ upstream of the bottleneck.

A long off ramp parallel to the other highway lanes can also play the role of a bottleneck of this type. This case is realized on the highway A5-South at $D12$, $D13$ [Fig. 3(a)]. Due to the off ramp the effective number of the lanes decreases from $m=4$ at $D12$ to $n=3$ at $D14$ in the direction of traffic flow. Apparently for this reason the width of the foreign wide moving jam in Fig. 25(c) decreases when the jam propagates upstream in the vicinity of $D12$ and $D13$ and the jam width again increases after the jam has passed the off ramp [this is the wide moving jam shown in Fig. 2(b)].

The influence of this long off ramp at $D12$, $D13$ can also explain the dissolution of narrow moving jams shown in Fig. 25(d). These jams emerge in the pinch region of the congested pattern [$D14$, Fig. 25(d)] that appears upstream of the effective bottleneck at $D16$ caused by the on ramp $D15$-on in Fig. 3(a). After this moving jam dissolution, free flow occurs upstream of the pinch region at $D12$ [Fig. 25(d)]. Thus, the localized synchronized flow pattern occurs at the on ramp [this pattern is marked as synchronized flow in Fig. 2(b)] rather than the general pattern. However, in contrast to LSP considered in Sec. IV B (Fig. 19), the localized synchronized flow pattern under consideration [Figs. 2(b) and 25(d)] occurs due to the mentioned peculiarities of the highway infra-

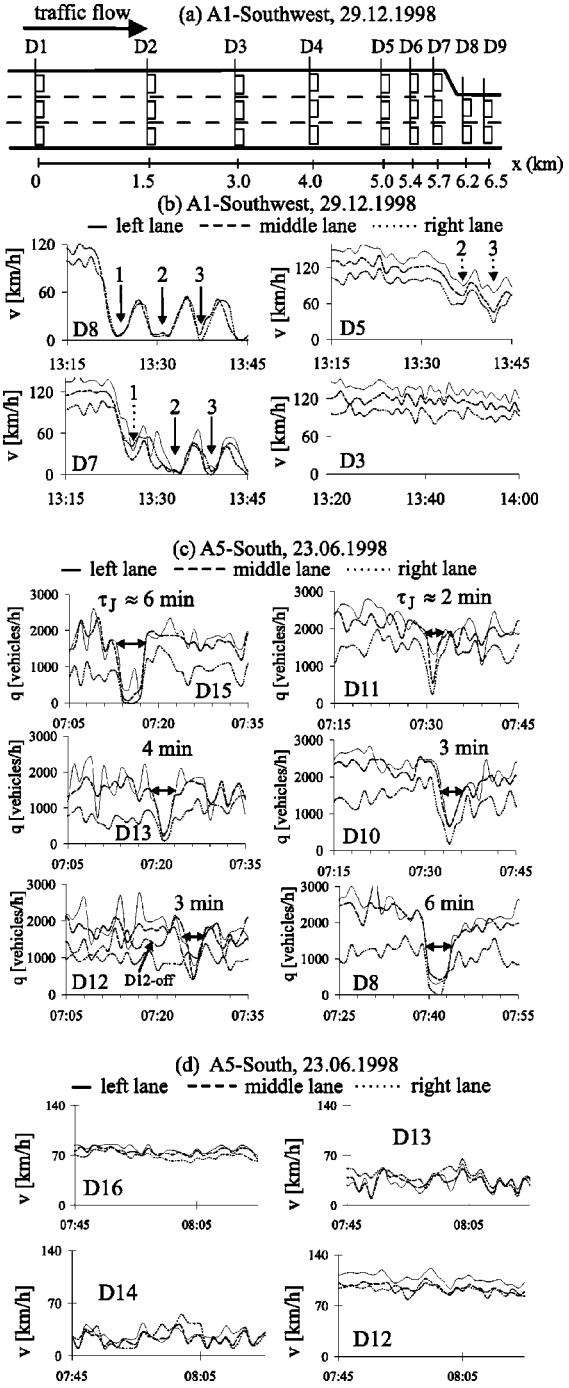

FIG. 25. Dissolution of moving jams at bottlenecks. (a, b) A scheme of the arrangement of the detectors on the section of the highway A1-Southwest between intersection "Dortmund-Unna" (upstream of $D1$) and intersection "Schwerte" (downstream of $D9$) in the direction to Cologne (a) and the vehicle speed at different detectors (b). (c) Dependence of the time-width τ_J of a wide moving jam due to the jam propagation through a section of the highway A5-South with the long off ramp [$D12$ and $D13$, Fig. 3(a)]: the vehicle speed at different detectors. (d) Dissolution of narrow moving jams occurring in the pinch region ($D14$) of the localized synchronized flow pattern due to the jam propagation through a part of the section of the highway A5-South with the long off ramp: the vehicle speed at different detectors.

structure upstream of the effective bottleneck at $D16$ rather than due to non linear effects in traffic upstream of the bottleneck only.

VII. DISCUSSION

A. Conclusions of empirical results

1. Classification of congested patterns at highway bottlenecks

(i) GP, where the synchronized flow occurs and wide moving jams emerge in that synchronized flow is the most frequent type of congested pattern at isolated bottlenecks.

(ii) In some cases, rather than GP one of the SP's occurs. Either LSP, or WSP, or else MSP is realized at an isolated bottleneck.

(iii) In some cases in GP and SP (in LSP and WSP) local regions of free flow, which spatially alternate with regions of synchronized flow, can occur.

(iv) If two or more effective bottlenecks are close to one another, EP, where synchronized flow covers two or more effective bottlenecks, can occur.

For each effective bottleneck or for each set of several effective bottlenecks that are close to one another the spatial-temporal structure of the congested patterns possesses predictable, i.e., characteristic, unique, and reproducible features, such as the types of patterns that are frequently formed and the mean width of synchronized flow inside GP. These features can be nearly *the same* for different days and years. They can also remain within a large range of flow rates (traffic demand) at which the patterns exist. These results are used for forecasting of congested patterns at highway bottlenecks [80].

2. Special congested pattern features

(i) When the flow rate to the effective on ramp $q_{eff\text{-}on}$ increases, the case of the strong congestion can be realized. The strong congestion shows the following features.

(1) The average flow rate in the pinch region of GP $q^{(pinch)}$ reaches a limit (minimal) flow rate $q_{lim}^{(pinch)}$. Exactly, $q^{(pinch)}$ shows only small changes in the vicinity of $q_{lim}^{(pinch)}$.

(2) The mean width of synchronized flow in GP, L_{syn}, is approximately a constant, which does not change if either the flow rate $q_{eff\text{-}on}$ or/and the flow rate upstream of GP q_{in} increases.

(3) At the location inside the pinch region where narrow moving jams are just emerging the time distance between the jams reaches a minimum value.

(4) The condition $q_{lim}^{(pinch)} < q_{out}$ is fulfilled ($1.2 \lesssim q_{out}/q_{lim}^{(pinch)} \lesssim 1.5$), where q_{out} is the flow rate in the outflow from a wide moving jam for the case when free flow is formed downstream of the jam.

(5) The highway capacity in the free flow regime can be about twice as high as the capacity of the highway under the strong congestion condition.

(ii) When the flow rate to the effective on ramp $q_{eff\text{-}on}$ slowly decreases, the strong congestion conditions in GP changes to the weak one. In this case, GP can transform into one of the SP or an alternation of free and synchronized flows in GP occurs.

(iii) In contrast to the strong congestion, under the weak one the flow rate $q^{(pinch)}$ or/and L_{syn} or/and the time-distance of the narrow moving jams emergence in a synchronized flow noticeably depend on traffic demand. In GP where in the pinch region the weak congestion occurs, the upstream front (boundary) of synchronized flow can propagate upstream, i.e., L_{syn} can continuously increase.

(iv) Under the weak congestion diverse transformations between different types of congested patterns can occur over time.

(v) At an isolated off ramp, the weak congestion is often observed.

(vi) Moving jams can dissolve at some specific bottlenecks. This effect can lead to the occurrence of LSP where the strong congestion in synchronized flow is realized, however in contrast to GP, the region of wide moving jams is absent.

(vii) The period of the speed correlation function can gradually increase in the upstream direction from the location in the pinch region where narrow moving jams are just emerging.

B. A qualitative explanation of empirical results

1. Diagram of congested patterns at bottlenecks in three-phase-traffic theory

The methodology of the congested pattern study that has been used above is based on an analysis of *empirical spatial-temporal* features of congested patterns. Let us show that some of these empirical features can be explained in the frame of three-phase-traffic theory by the author [57,62–64,66,81].

In the diagram of congested patterns at the bottlenecks (e.g., on and off ramps) on a multilane (in one direction) highway [Fig. 26(a)] [76,81], which is based on the three-phase-traffic theory [Figs. 26(b,c)] [57,62–64,66], different spatial-temporal congested patterns dependent on the flow rate on the highway upstream of the bottleneck q_{in} and on ''the effective bottleneck strength'' (or the bottleneck strength for short), Δq, are possible. If the effective bottleneck is caused by an on ramp, the bottleneck strength Δq equals the flow rate to the on ramp $q_{on\text{-}ramp}$ [Fig. 26(a)]. If the effective bottleneck is caused by an off ramp, Δq equals the difference between the actual flow rate to the off ramp and a threshold flow rate to the off ramp at which the off ramp still does not cause a permanent disturbance for free flow.

In the diagram, there are two main boundaries $F_S^{(B)}$ and $S_J^{(B)}$. Below and left of the boundary $F_S^{(B)}$ free flow is realized [Fig. 26(a)]. Between the boundaries $F_S^{(B)}$ and $S_J^{(B)}$ different SP's occur. Right of the boundary $S_J^{(B)}$ wide moving jams spontaneously emerge in synchronized flow upstream of the bottleneck, i.e., different GP's occur.

Between the boundaries $F_S^{(B)}$ and $S_J^{(B)}$, the higher q_{in} is, the higher is the probability that the flow rate in synchronized flow in SP is lower than q_{in} and the length of SP is continuously increasing over time. At higher q_{in} the WSP and at lower q_{in} the LSP occurs [Fig. 26(a)]. The boundary

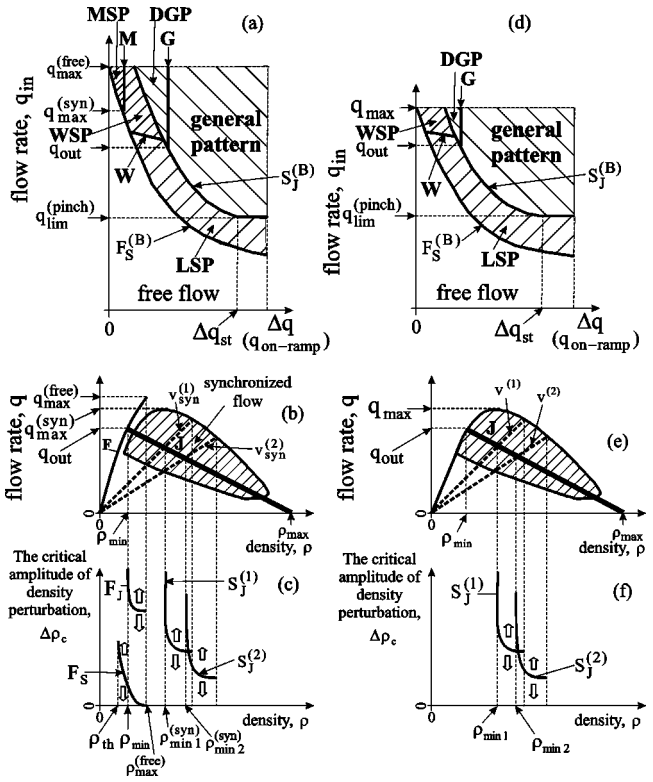

FIG. 26. A qualitative explanation of empirically found congested patterns in the three-phase-traffic theory. (a) A qualitative diagram of congested patterns at the effective isolated bottleneck on a multilane highway [76,81]: GP is the general pattern, DGP is the dissolving GP, LSP is the localized synchronized flow pattern, WSP is the widening synchronized flow pattern, MSP is the moving synchronized flow pattern; q_{in} is the flow rate on highway upstream of the bottleneck, Δq is the bottleneck strength, in the case of the bottleneck caused by the on ramp $\Delta q = q_{on\text{-}ramp}$. (b) A concatenation of hypothetical equilibrium states of free (F) and synchronized flow (dashed area) with the line J; (c) hypothetical critical amplitude of local perturbations as function of the density for the $F \rightarrow S$ transition (curve F_S), for the $F \rightarrow J$ transition (curve F_J), and for the $S \rightarrow J$ transition (curves $S_J^{(1)}$ and $S_J^{(2)}$ for two different vehicle speeds in synchronized flow $v_{syn}^{(1)}$ and $v_{syn}^{(2)}$, respectively, $v_{syn}^{(1)} > v_{syn}^{(2)}$) [57,63,66]. A qualitative diagram of congested patterns (d), a concatenation of hypothetical equilibrium flow states with the line J (e), and hypothetical critical amplitude of local perturbations as function of the density for the $S \rightarrow J$ transition (curves $S_J^{(1)}$ and $S_J^{(2)}$ for two different vehicle speeds $v^{(1)}$ and $v^{(2)}$, respectively, $v^{(1)} > v^{(2)}$) (f) for one-lane road.

that separates the region of WSP from the region of LSP is marked by the letter W in Fig. 26(a).

Note that the flow rate in the synchronized flow of any SP cannot exceed some characteristic value $q_{max}^{(syn)}$ [Fig. 26(b)]. Right of the boundary $F_S^{(B)}$ and left of the line M [the region marked ''MSP'' in Fig. 26(a)] the flow rate q_{in} in an initial free flow upstream of the on ramp satisfies the condition $q_{in} > q_{max}^{(syn)}$ [Fig. 26(a)]. The point where the line M intersects the curve $F_S^{(B)}$ is related to the flow rate $q_{in} = q_{max}^{(syn)}$. After SP has just appeared at the on ramp, the flow rate directly upstream of the on ramp decreases. This flow rate in SP pinned at the on ramp cannot be higher than $q_{max}^{(syn)}$. This

is in contrast to the initial condition $q_{in} > q_{max}^{(syn)}$. Apparently for this reason, it has been found out [76] that one or a sequence of MSP emerge upstream of the on ramp. After SP has emerged at the on ramp, SP comes off the on ramp and transforms into MSP. In MSP both the upstream and the downstream fronts move upstream of the on ramp, i.e., MSP moves as a whole localized pattern upstream of the on ramp. In contrast to a wide moving jam, inside MSP both the vehicle speed (40–70 km/h) and the flow rate are high. Besides, the velocity of the downstream front of MSP is not a characteristic parameter. This velocity can change in a wide range in the process of the MSP propagation or for different MSP. In some cases it has been found out that after MSP is far away from the on ramp, the pinch effect (the self-compression of synchronized flow) occurs inside MSP and a wide moving jam can be formed there [76].

The boundary $F_S^{(B)}$ [Fig. 26(a)] is determined by an occurrence of the $F \rightarrow S$ transition at the bottleneck. The nature of this boundary is similar to the one for the curve F_S in Fig. 26(c), which determines the critical amplitude of local perturbations for the $F \rightarrow S$ transition in traffic flow without bottlenecks [62,63]. The effective bottleneck acts as a permanent nonhomogeneity that causes the related permanent perturbation at the bottleneck [67]. The higher Δq is, the higher is the amplitude of this permanent perturbation. Therefore, the higher Δq is the lower is the flow rate q_{in} at which the related critical amplitude occurs at the bottleneck. This may explain the decreasing character of the boundary $F_S^{(B)}$ in the flow-flow plane in Fig. 26(a). The limit point of the boundary $F_S^{(B)}$ at $\Delta q = 0$ is related to the maximum flow rate in free flow where $q_{in} = q_{max}^{(free)}$.

The boundary $S_J^{(B)}$ is determined by the wide moving jam emergence in synchronized flow (i.e., the $S \rightarrow J$ transition) upstream of the on ramp. The nature of the boundary $S_J^{(B)}$ is similar to the one for the curves $S_J^{(1)}$ and $S_J^{(2)}$ in Fig. 26(c). The latter boundaries determine the critical amplitude of local perturbation and the related probability for the $S \rightarrow J$ transition in synchronized flow [57,62,63,66]. On the one hand, between the boundaries $F_S^{(B)}$ and $S_J^{(B)}$, at the same q_{in} the vehicle speed in SP should decrease when Δq increases. On the other hand, from Figs. 26(b,c) it can be seen that at the same flow rate q, the lower the vehicle speed in synchronized flow, the lower is the critical amplitude $\Delta \rho_c$ and therefore the higher is the probability of the $S \rightarrow J$ transition (compare $S_J^{(1)}$ and $S_J^{(2)}$ for the respective vehicle speeds $v_{syn}^{(1)}$ and $v_{syn}^{(2)}$, where $v_{syn}^{(1)} > v_{syn}^{(2)}$). Thus, in comparison to $F_S^{(B)}$, the boundary $S_J^{(B)}$ should be shifted to the right in the flow-flow plane [Fig. 26(a)].

The empirical results of the GP formation also allow to suggest that if due to the high value of Δq the strong congestion is achieved in GP, then GP cannot exist if $q_{in} < q_{lim}^{(pinch)}$. Therefore, under the strong congestion the boundary $S_J^{(B)}$ can transform into a horizontal line at $q_{in} = q_{lim}^{(pinch)}$ [Fig. 26(a)]. However, it can also occur that at the whole boundary $S_J^{(B)}$ the flow rate $q_{in} > q_{lim}^{(pinch)}$, i.e., the boundary $S_J^{(B)}$ has a decreasing character at all values q_{in} and Δq in the flow-flow plane. In this case, either the part of the diagram of congested patterns in Fig. 26(a), which is related to the values $\Delta q \geqslant \Delta q_{st}$, is not realized or the whole boundary $S_J^{(B)}$ lies above the flow rate $q_{in} = q_{lim}^{(pinch)}$.

Right of the boundary $S_J^{(B)}$ and left of the line G [the region marked ''DGP (dissolving general pattern)'' in Fig. 26(a)], in an initial (before the congested pattern formation) free flow upstream of the on ramp, the flow rate q_{in} satisfies the condition $q_{in} > q_{out}$. The point where the line G intersects the curve $S_J^{(B)}$ is related to the flow rate $q_{in} = q_{out}$. Thus, after a wide moving jam in synchronized flow of the congested pattern has been formed, this initial condition $q_{in} > q_{out}$ cannot be satisfied anymore because the flow rate in the jam outflow cannot be higher than q_{out}. As a result, DGP, i.e., GP that dissolves over time should occur [Fig. 26(a)]. As a result, GP transforms into one of the SP or free flow occurs at the bottleneck [76].

Right of the boundary $S_J^{(B)}$ and right of the line G, GP occurs [Fig. 26(a)]. As well as in the empirical results presented above, GP does *not* transform into another type of pattern if Δq increases. If Δq decreases, GP can transform into one of SP.

The diagram in Fig. 26(a) [76,81] can also explain the occurrence of the diverse variety of patterns and the transformations between them over time under the weak congestion at off ramps. Indeed, the weak congestion should be related to lower Δq, i.e., to the part of the diagram in Fig. 26(a) where even relatively small changes in q_{in} and Δq can cause diverse transitions between MSP, WSP, GP, DGP, and free flow.

Note that for a one-lane road the diagram of congested patterns should be qualitatively similar to that for the multilane highway with one exception. The part of the diagram above the flow rate $q_{in} = q_{max}^{(syn)}$ in Fig. 26(a) is not realized on the diagram of congested patterns for the one-lane road [Fig. 26(d)]. This is linked to the hypotheses of the three-phase-traffic theory [Figs. 26(e,f)] [57,62,63,66]. Indeed, these hypotheses suggest that the maximal flow rate q_{max} [Fig. 26(e)] in hypothetical spatially homogeneous and time-independent states (''equilibrium'' states) on the one-lane road equals the maximal flow rate in the related states of synchronized flow on the multilane highway: $q_{max} = q_{max}^{(syn)}$ [Figs. 26(b,e)]. Therefore, corresponding to Fig. 26(d) MSP should not occur at a bottleneck on the one-lane road.

In Figs. 26(a,d) fluctuations and hysteresis effects have not been taken into account. Fluctuations may lead to the $S \rightarrow F$ transition inside WSP, and in particular to an occurrence of MSP also on one-lane roads. Hysteresis effects may lead to an appearance of regions where, dependent on initial conditions, several different patterns can occur. In particular, the region of solely MSP may ''shrink'' so that in a limit case in the whole region marked ''MSP'' in Fig. 26(a) WSP can exist on a multi-lane road. The region of solely DGP may also ''shrink'' and in a limit case GP can exist at all values q_{in} right of the boundary $S_J^{(B)}$.

2. Comparison with the diagram of congested patterns at bottlenecks in the fundamental diagram approach

Traffic flow models use usually hypothetical spatial homogeneous and time-independent states (''equilibrium''

states or fixed points of a model) that belong to a curve(s) in the flow-density plane—the fundamental diagram approach (e.g., Refs. [13–15,27,28,30,51,52]). Helbing *et al.* [38,41,52] have derived a diagram of congested patterns at bottlenecks for a wide class of models in the frame of the fundamental diagram approach, where diverse congested patterns are possible depending on the flow rate q_{in} and on the bottleneck strength Δq (the term ''the bottleneck strength'' has been introduced in Refs. [38,41,52]). This diagram [38,41,52] is qualitatively different from the diagrams in Figs. 26(a,d) [76,81].

(i) In the diagram based on the fundamental diagram approach [38,41,52], homogeneous congested patterns (HCT) occur at very *high* flow rates to the on ramp $q_{on\text{-}ramp}$ (in the general case, the bottleneck strength Δq) *only*. In contrast, in Figs. 26(a,d) [76], WSP, where as in HCT synchronized flow can be homogeneous can occur in the vicinity of *low* $q_{on\text{-}ramp}$ *only*.

(ii) In Refs. [38,41,52], at a given high enough q_{in} if the flow rate $q_{on\text{-}ramp}$ continuously increases first triggered stop-and-go traffic (TSG) where no synchronized flow can be formed occurs, then oscillating patterns (OCT) where no wide moving jams can be formed appear, and finally HCT occurs. In contrast, in the diagrams in Figs. 26(a,d) [76,81] there are neither TSG or OCT, nor HCT.

(iii) Near the boundary that separates TSG and OCT a congested pattern that is a ''mixture'' of TSG and OCT (and HCT) can occur [52]. This pattern, which at first sight looks like GP, has been used in Ref. [52] for an explanation of the jam emergence in Ref. [66]. However, this mixture pattern has no own region in the diagram of states in Refs. [38,41,52]: The pattern transforms into TSG if $q_{on\text{-}ramp}$ decreases or into OCT if $q_{on\text{-}ramp}$ increases. In our diagrams [Figs. 26(a,d) [76,81]] there are no TSG, no OCT, and no HCT. Instead, GP exists in the very large range of the flow rates $q_{on\text{-}ramp}$ and q_{in}. At a given q_{in} GP in the three-phase-traffic theory does not transform into another congested pattern even if $q_{on\text{-}ramp}$ increases up to the highest possible values. Thus GP in Fig. 26(a) [76,81] has a qualitatively different nature in comparison with the mixture of TSG and OCT (and HCT) in Ref. [52].

(iv) In Refs. [38,41,52], if $q_{on\text{-}ramp}$ decreases, then dependent on q_{in}, either PLC or TSG, i.e., either a pinned jam or moving jams of very high density and very low speed occur. This is also in contrast to the diagrams in Figs. 26(a,d) [76,81]. If $q_{on\text{-}ramp}$ decreases, SP occurs where the density is much lower and the speed is much higher than that inside either synchronized flow of the general pattern or inside any jams (for more detailed comparison see Ref. [76]).

The theoretical diagram of states in the fundamental diagram approach [38,41,52] predicts the following sequence of the congested pattern transformation if $q_{on\text{-}ramp}$ gradually increases. (i) TSG→OCT→HCT at a high given flow rate q_{in} and (ii) PLC→OCT→HCT at a lower given q_{in}. These sequences (or even a part of them) have *not* been observed in the study of congested patterns presented in the paper. In contrast, GP usually spontaneously emerges at the on ramp. GP does not transform into another congested pattern if $q_{on\text{-}ramp}$ increases. If $q_{on\text{-}ramp}$ decreases, GP transforms into SP where vehicle speed is considerably higher than in the synchronized flow of GP. This is in accordance with the diagram in Fig. 26(a) in the three-phase-traffic theory [63,64,66,76,81].

3. The width of synchronized flow in GP under the strong congestion

It can be assumed that a wide moving jam separates the traffic flows upstream and downstream of the jam. As long as a moving jam is the wide one traffic phenomena upstream of the jam do not depend on traffic phenomena downstream of the jam.

In the strong congestion condition, the wide moving jam at the upstream boundary of synchronized flow in GP can therefore be considered as a region where ''superfluous'' vehicles that cannot immediately pass through the pinch region are virtually stored. The average flow rate upstream of the wide moving jam q_{in} is assumed to be higher than the flow rate $q_{lim}^{(pinch)}$ [Fig. 26(a)]. Due to the difference between q_{in} and $q_{lim}^{(pinch)}$ the width of the jam increases only. In other words, there is no influence on the width L_{syn} and on other parameters of synchronized flow downstream of the jam even if q_{in} is for a long time considerably higher than the capacity of the congested bottleneck.

It can be assumed that

$$L_{syn}=|v_{narrow,\,mean}|T_{narrow}, \tag{9}$$

where $v_{narrow,\,mean}$ is the mean velocity of narrow jams and T_{narrow} is the mean time interval needed for the transformation of the narrow jams into the wide jams.

In some time after the general pattern has been formed, more than one wide moving jam usually exist upstream of the pinch region. In the strong congestion condition, if the flow rate upstream of the region of these wide moving jams $q_{in}>q_{lim}^{(pinch)}$, the changes in q_{in} do not influence the width L_{syn} either. An increase in traffic demand q_{in} leads to the related increase in the width of the most upstream wide moving jam.

When in contrast q_{in} becomes during a long time noticeably lower than q_{out}, wide moving jams that are far away from the upstream boundary of synchronized flow will disappear. Then, if q_{in} becomes lower than $q_{lim}^{(pinch)}$ the strong congestion at the bottleneck dissolves also.

4. Remarks about unsolved problems

In empirical observations, synchronized flow shows a very complex dynamical behavior. This may explain why there is no common view on the physics and on the nature of synchronized flow between different scientific groups up to now (e.g., the discussion in the review by Helbing [52] and in Sec. VII B 2). This also explains why new diverse qualitatively different traffic flow models and theories for a theoretical description of synchronized flow appeared during the last years (e.g., [36–40,42–44,47–50,52,61,74–76,82–86]). In particular, the behavior and the role of fluctuations in comparison with deterministic effects and also features of critical fluctuations in synchronized flow leading to the mov-

ing jam emergence have not been sufficiently understood. Thus, these and many other unsolved problems linked to synchronized flow features is a very interesting and important field of future investigations.

C. Application of the results for the development of methods for tracing and forecasting of congested patterns

The three-phase-traffic theory [57,63,64,66,76,81] that has been used for a qualitative explanation of empirical results has also been confirmed by the online application in the traffic center of the State Hessen of some recent models ''ASDA'' (automatische Staudynamikanalyse: automatic tracing of moving traffic jams) [87,88] and ''FOTO'' (forecasting of traffic objects) [89,90], which are based on this traffic flow theory. The model ASDA performs the automatic tracing and prediction of the propagation of moving traffic jams. The model FOTO identifies the traffic phases and performs the tracing and prediction of the traffic phase synchronized flow. It must be noted that in contrast to the conventional model approach based on microscopic, mesoscopic, or macroscopic traffic flow models (e.g., Ref. [29]), the models ASDA and FOTO perform without any validation of model parameters in different environmental and traffic conditions.

In the approach [87–90], first the initial fronts of moving jams $x_{up}^{(jam)}$, $x_{down}^{(jam)}$ and of synchronized flow $x_{up}^{(syn)}$, $x_{down}^{(syn)}$ are determined. These fronts define the spatial size and location of the phases synchronized flow and wide moving jam. Then the tracing and forecasting of the fronts of these phases in time and space is calculated, i.e., the positions of all fronts $x_{up}^{(jam)}(t)$, $x_{down}^{(jam)}(t)$, $x_{up}^{(syn)}(t)$, $x_{down}^{(syn)}(t)$ as functions of time are found. Note that for the traffic forecasting historical time series at least for the flow rates are necessary. In other words, after the recognition of the traffic phases in congested regime, these phases are traced and predicted as macroscopic single objects. The knowledge of these parameters as well as the average vehicle speed inside the traffic phases allow to calculate other traffic characteristics, e.g., trip times or/and vehicle trajectories.

The field tests of the models ASDA and FOTO [91] show that the dynamics of the traffic phases synchronized flow and wide moving jam in the three-phase-traffic theory can describe the real pattern dynamics almost exactly [Fig. 27(a)]. The output information of ASDA and FOTO can be used for driver information systems or for traffic control systems. It is also possible to predict the dissolution of moving jams and of patterns of synchronized flow.

For the evaluation of the model results, empirical data of an infrastructure with many detectors have been chosen. First, the data of all detectors have been used [Fig. 27(b)]. Then, the data of some detectors have been omitted and the process of the traffic pattern recognition and prediction has been repeated [Fig. 27(c)]. The data that have not been used are taken for comparison to the model results. The histogram where instead of 31 detection sites only 9 detection sites are used [Fig. 27(c)] shows a very similar result at the same situation as in Fig. 27(b) with all detectors as input.

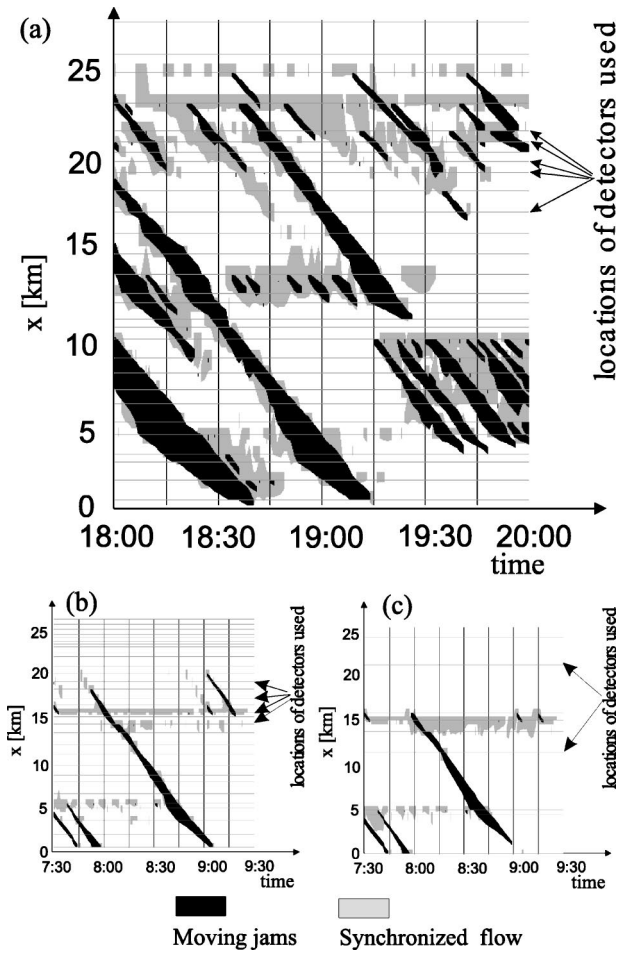

FIG. 27. Results of the online application of the model ASDA and FOTO. (a) Histogram A5-North on 12 April 2000 from 18:00–20:00. Histogram A5-South on 17 July 2000 from 07:30–09:30 using all available traffic data (31 sets of the detectors) (b) and the same day and the time interval as in (b) but using reduced input data (9 of 31 sets of the detectors are used) (c).

ACKNOWLEDGMENTS

I thank Hubert Rehborn, Sergey Klenov, Mario Aleksic, and Andreas Haug for their help and the discussion; Hessisches Landesamt für Straßen und Verkehrswesen Frankfurt for support in the preparation of the data; and the German Ministry of Education and Research for financial support within the BMBF project ''DAISY.''

[1] M.J. Lighthill and G.B. Whitham, Proc. R. Soc. London, Ser. A **229**, 317 (1955).

[2] D.C. Gazis, R. Herman, and R.W. Rothery, Oper. Res. **9**, 545 (1961).

[3] R. Herman, E.W. Montroll, R.B. Potts, and R.W. Rothery, Oper. Res. **7**, 86 (1959).

[4] G.F. Newell, Oper. Res. **9**, 209 (1961).

[5] I. Prigogine and R. Herman, *Kinetic Theory of Vehicular Traf-*

fic (American Elsevier, New York, 1971).
[6] H.J. Payne, in *Mathematical Models of Public Systems*, edited by G.A. Bekey (Simulation Council, La Jolla, 1971, Vol. 1).
[7] R. Wiedemann, *Simulation des Verkehrsflusses* (University of Karlsruhe, Karlsruhe, 1974).
[8] P.G. Gipps, Transp. Res., Part B: Methodol. **15**, 105 (1981).
[9] G.F. Newell, *Applications of Queuing Theory* (Chapman Hall, London, 1982).
[10] C. F. Daganzo, *Fundamentals of Transportation and Traffic Operations* (Elsevier, New York, 1997).
[11] *Transportation and Traffic Theory*, Proceedings of the 13th International Symposium on Transportation and Traffic Theory, edited by J.-B. Lesort (Elsevier, Oxford, 1996).
[12] *Transportation and Traffic Theory*, Proceedings of the 14th International Symposium on Transportation and Traffic Theory, edited by A. Ceder (Elsevier, Oxford, 1999).
[13] *Traffic and Granular Flow*, Proceedings of the International Workshop on Traffic and Granular Flow, 1995, edited by D. E. Wolf, M. Schreckenberg, and A. Bachem (World Scientific, Singapore, 1995).
[14] *Traffic and Granular Flow' 97*, Proceedings of the International Workshop on Traffic and Granular Flow, 1997, edited by M. Schreckenberg, and D. E. Wolf (Springer, Singapore, 1998).
[15] *Traffic and Granular Flow' 99*, Proceedings of the International Workshop on Traffic and Granular Flow, 1999, edited by D. Helbing, H. J. Herrmann, M. Schreckenberg, and D. E. Wolf (Springer, Heidelberg, 2000).
[16] K. Nagel and M. Schreckenberg, J. Phys. I **2**, 2221 (1992).
[17] G.B. Whitham, Proc. R. Soc. London, Ser. A **428**, 49 (1990).
[18] M. Bando, K. Hasebe, A. Nakayama, A. Shibata, and Y. Sugiyama, Phys. Rev. E **51**, 1035 (1995).
[19] B.S. Kerner and P. Konhäuser, Phys. Rev. E **50**, 54 (1994).
[20] M. Herrmann and B.S. Kerner, Physica A **255**, 163 (1998).
[21] M. Bando, K. Hasebe, A. Nakayama, A. Shibata, and Y. Sugiyama, J. Phys. I **5**, 1389 (1995).
[22] S. Krauß, P. Wagner, and C. Gawron, Phys. Rev. E **55**, 5597 (1997).
[23] R. Barlovic, L. Santen, A. Schadschneider, and M. Schreckenberg, Eur. Phys. J. B **5**, 793 (1998).
[24] D. Helbing and M. Schreckenberg, Phys. Rev. E **59**, R2505 (1999).
[25] M. Treiber, A. Hennecke, and D. Helbing, Phys. Rev. E **59**, 239 (1999).
[26] R. Mahnke and J. Kaupužs, Phys. Rev. E **59**, 117 (1999).
[27] G.B. Whitham, *Linear and Nonlinear Waves* (Wiley, New York, 1974).
[28] A.D. May, *Traffic Flow Fundamental* (Prentice-Hall, New Jersey, 1990).
[29] M. Cremer, *Der Verkehrsfluss auf Schnellstrassen* (Springer, Berlin, 1979).
[30] W. Leutzbach, *Introduction to the Theory of Traffic Flow* (Springer, Berlin, 1988).
[31] D. Helbing, *Verkehrsdynamik* (Springer, Berlin, 1997).
[32] R. Kühne, in *Highway Capacity and Level of Service*, edited by U. Brannolte (A. A. Balkema, Rotterdam, 1991), p. 211.
[33] K. Nagel, D.E. Wolf, P. Wagner, and P. Simon, Phys. Rev. E **58**, 1425 (1999).
[34] B.S. Kerner, S.L. Klenov, and P. Konhäuser, Phys. Rev. E **56**, 4200 (1997).
[35] B.S. Kerner, P. Konhäuser, and M. Schilke, Phys. Rev. E **51**, 6243 (1995).
[36] H.Y. Lee, H.-W. Lee, and D. Kim, Phys. Rev. Lett. **81**, 1130 (1998).
[37] D. Helbing and M. Treiber, Phys. Rev. Lett. **81**, 3042 (1998).
[38] D. Helbing, A. Hennecke, and M. Treiber, Phys. Rev. Lett. **82**, 4360 (1999).
[39] M. Treiber and D. Helbing, J. Phys. A **32**, L17 (1999).
[40] H.Y. Lee, H.-W. Lee, and D. Kim, Phys. Rev. E **59**, 5101 (1999).
[41] M. Treiber, A. Hennecke, and D. Helbing, Phys. Rev. E **62**, 1805 (2000).
[42] H.Y. Lee, H.-W. Lee, and D. Kim, Physica A **281**, 78 (2000); Phys. Rev. E **62**, 4737 (2000).
[43] E. Tomer, L. Safonov, and S. Havlin, Phys. Rev. Lett. **84**, 382 (2000).
[44] H.M. Zhang and T. Kim, in *Proceedings of the Preprints of the 80th TRB Annual Meeting, Washington D.C., 2001* (TRB, Washington D.C., 2001).
[45] A. Klar and R. Wegener, SIAM (Soc. Ind. Appl. Math.) J. Appl. Math. **59**, 983 (1999); **59**, 1002 (1999).
[46] J.H. Banks, Transp. Res. Rec. **1678**, 128 (1999).
[47] P. Nelson, Phys. Rev. E **61**, R6052 (2000).
[48] P. Nelson and Z. Hu, in *Traffic and Transportation Studies*, Proceedings of ICTTS 2000, Beijing, People's Republic of China, 2000, edited by K.C.P. Wang, G. Xiao, and J. Ji (ASCE, Reston, Virgina, 2000), pp. 594–601.
[49] I. Lubashevsky and R. Mahnke, Phys. Rev. E **62**, 6082 (2000).
[50] M. Krbalek, P. Šeba, and P. Wagner, Phys. Rev. E **64**, 066119 (2001).
[51] D. Chowdhury, L. Santen, and A. Schadschneider, Phys. Rep. **329**, 199 (2000).
[52] D. Helbing, Rev. Mod. Phys. **73**, 1067 (2001).
[53] J. Treiterer, Ohio State University Technical Report No. PB 246 094, Columbus, Ohio, 1975 (unpublished).
[54] M. Koshi, M. Iwasaki, and I. Ohkura, in *Proceedings of 8th International Symposium on Transportation and Traffic Theory*, edited by V. F. Hurdle *et al.* (University of Toronto Press, Toronto, Ontario, 1983), p. 403.
[55] F.L. Hall, B.L. Allen, and M.A. Gunter, Transp. Res., Part A **20**, 197 (1986).
[56] B.S. Kerner and H. Rehborn, Phys. Rev. E **53**, R4275 (1996).
[57] B. S. Kerner, in *Proceedings of the 3rd Symposium on Highway Capacity and Level of Service*, edited by R. Rysgaard (Road Directorate, Ministry of Transport, Denmark, 1998), Vol. 2, pp. 621–642.
[58] B.S. Kerner and H. Rehborn, Phys. Rev. Lett. **79**, 4030 (1997).
[59] B. Persaud, S. Yagar, and R. Brownlee, Transp. Res. Rec. **1634**, 64 (1998).
[60] F.L. Hall, V.F. Hurdle, and J.H. Banks, Transp. Res. Rec. **1320**, 91 (1992).
[61] L. Neubert, L. Santen, A. Schadschneider, and M. Schreckenberg, Phys. Rev. E **60**, 6480 (1999).
[62] B.S. Kerner, in *Transportation and Traffic Theory*, edited by A. Ceder (Elsevier, Amsterdam, 1999), pp. 147–171.
[63] B.S. Kerner, Transp. Res. Rec. **1678**, 160 (1999).
[64] B.S. Kerner, Phys. World **12(8)**, 25 (1999).

[65] B. S. Kerner, in *Transportation Systems 1997*, edited by M. Papageorgiou and A. Pouliezos (Elsevier, London, 1997), pp. 765–770.
[66] B.S. Kerner, Phys. Rev. Lett. **81**, 3797 (1998).
[67] B.S. Kerner, Transp. Res. Rec. **1710**, 136 (2000).
[68] B. S. Kerner, in *Traffic and Granular Flow '99* (Ref. [15]), pp. 253–284.
[69] B.S. Kerner, J. Phys. A **33**, L221 (2000).
[70] B.S. Kerner and H. Rehborn, Phys. Rev. E **53**, R1297 (1996).
[71] B.S. Kerner and H. Rehborn, Internationales Verkehrswesen **50**, 196 (1998).
[72] B.S. Kerner, in *Traffic and Granular Flow '97* (Ref. [14]), p. 239–267.
[73] B.S. Kerner, Networks and Spatial Economics **1**, 35 (2001).
[74] W. Knospe, L. Santen, A. Schadschneider, and M. Schreckenberg, J. Phys. A **33**, L477 (2000).
[75] W. Knospe, L. Santen, A. Schadschneider, and M. Schreckenberg, Phys. Rev. E **65**, 015101(R) (2001).
[76] B.S. Kerner and S.L. Klenov, J. Phys. A **35**, L31 (2002).
[77] H. Haken, *Synergetics* (Springer, Berlin, 1997).
[78] B.S. Kerner and V.V. Osipov, *Autosolitons: A New Approach to Problems of Self-Organization and Turbulence* (Kluwer, Dordrecht, 1994).
[79] J.S. Bendat and A.G. Piersol, *Random Data. Analysis and Measurements Procedures* (Wiley, New York, 1986).
[80] B.S. Kerner, German Patent No. DE 199 44 075 (pending).
[81] B.S. Kerner, in *Proceedings of the Preprints of the Transportation Research Board 81 st Annual Meeting* (TRB, Washington D.C., 2002).
[82] D. Helbing, D. Batic, M. Schönhof, and M. Treiber, e-print cond-mat/0108548 (2001).
[83] S. Rosswog and P. Wagner, e-print cond-mat/0110101 (2001).
[84] S. Kriso, R. Friedrich, J. Peinke, and P. Wagner, e-print cond-mat/0110084 (2001).
[85] E. Tomer, L. Safonov, N. Madar, and S. Havlin, e-print cond-mat/0105493 (2001).
[86] I. Lubashevsky, R. Mahnke, P. Wagner, and S. Kalenkov, e-print cond-mat/0112139 (2001).
[87] B.S. Kerner, H. Rehborn, and H. Kirschfink, German Patent No. DE 196 47 127 (pending); U.S. Patent No. US 5861820 (19 January 1999).
[88] B.S. Kerner and H. Rehborn, German Patent No. DE 198 35 979 (pending).
[89] B.S. Kerner, M. Aleksic, and U. Denneler, German Patent No. DE 199 44 077 (pending).
[90] B.S. Kerner, H. Rehborn, M. Aleksic, and A. Haug, Traffic Eng. Control **42**, 282 (2001).
[91] B.S. Kerner, H. Rehborn, M. Aleksic, A. Haug, and R. Lange, Traffic Eng. Control **42**, 345 (2001).